Přehled technik – molekulová analýza

- **Reflexní techniky infračervené spektrometrie – ATR, DRIFT, IRRAS**
- Infračervená mikrospektroskopie

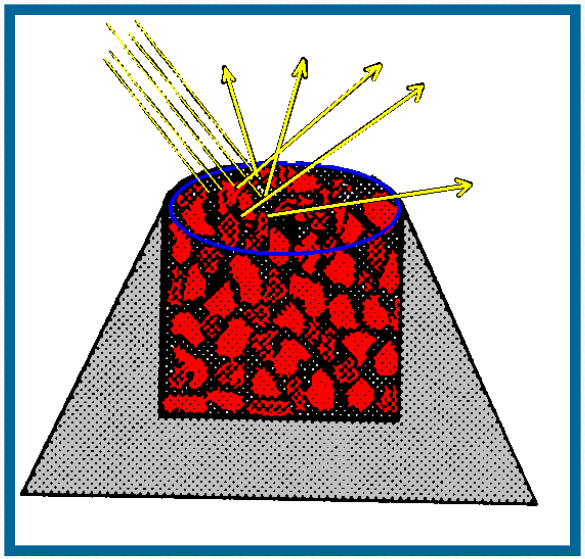

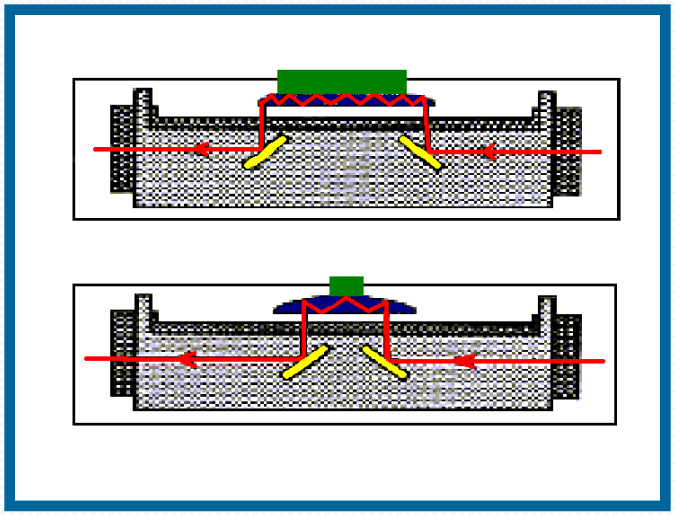

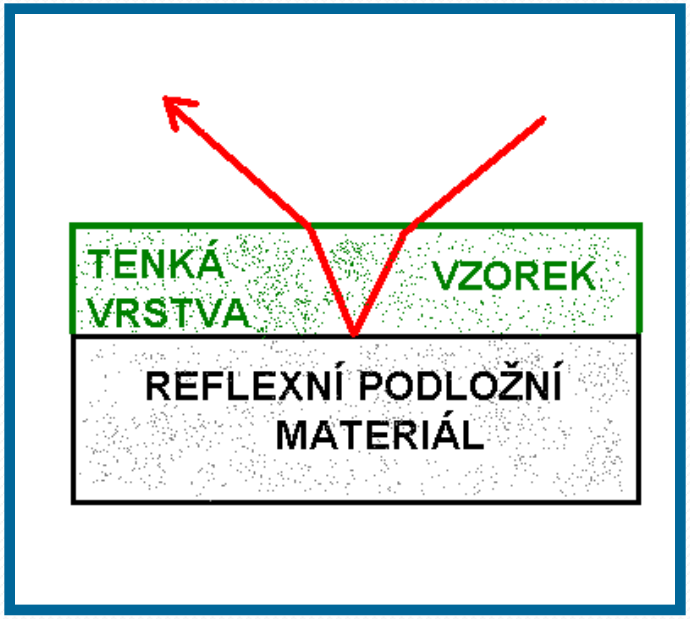

Infračervená spektrometrie

ANALYZOVANÉ TYPY MATERIÁLŮ

- plyny - analýza složení zemního plynu
  - monitoring vzdušných polutantů
- kapaliny, roztoky - analýza olejů
  - analýza odpadních vod
  - analýza mléka
- práškové vzorky - analýza léčiv, drog, trhavin
  - analýza rud, hnojiv
- fázové rozhraní - povrchová analýza

Infračervená spektrometrie - instrumentace

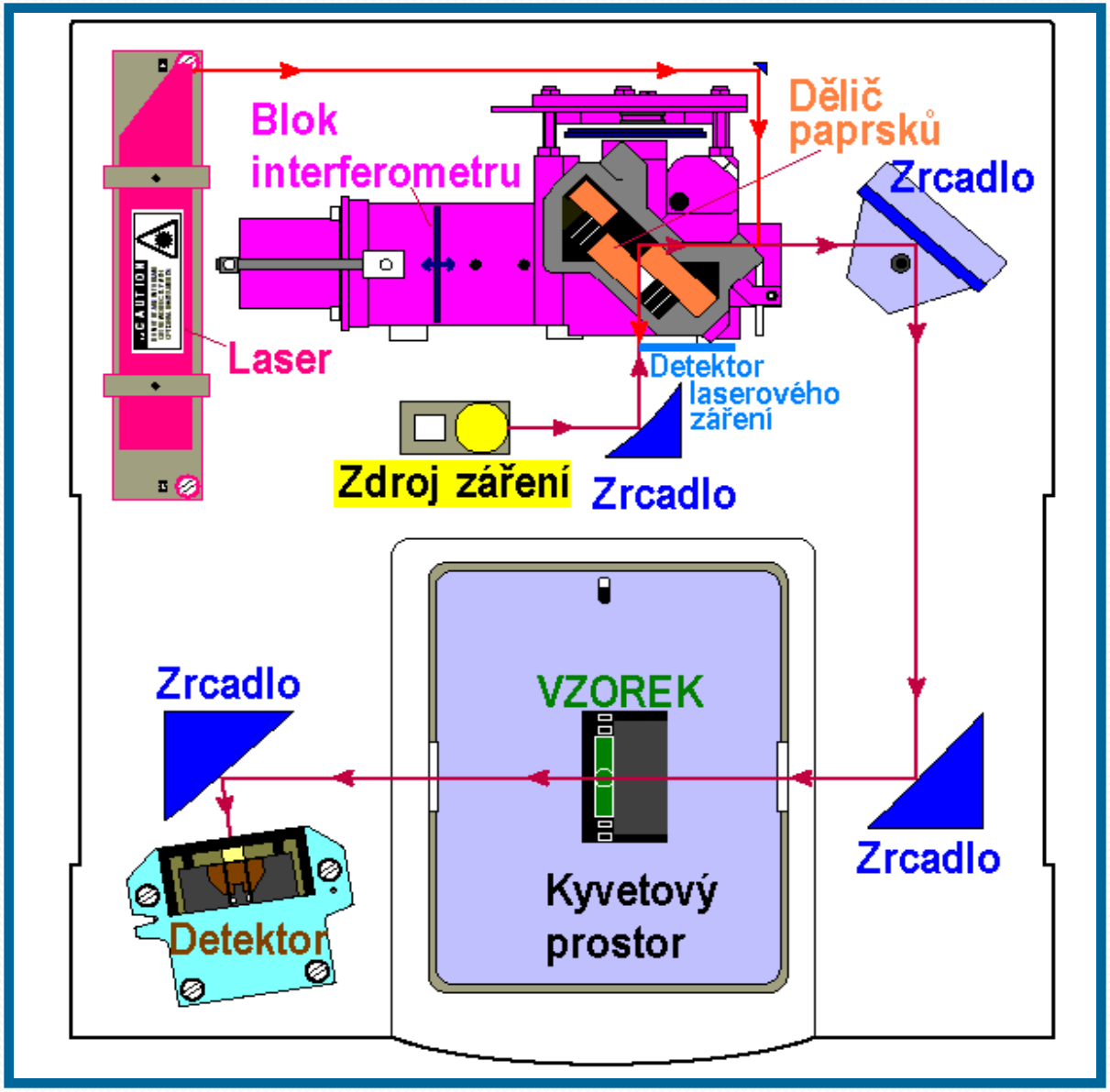

Infračervená spektrometrie

Oscilující dipólový moment

pohyb molekuly spojený se změnou elektrického dipolového momentu
vede k absorpci (nebo k emisi) záření

$$p = p_0 + \left(\frac{\partial p}{\partial q}\right)_0 q$$

p - aktuální dipólový moment

p_0 - dipólový moment v rovnovážné poloze

q - normální souřadnice vibračního módu

Infračervená spektrometrie

Základní výběrové pravidlo infračervené absorpce

$$\frac{\partial p}{\partial q} \neq 0$$

***INTENZITA PÁSŮ ÚMĚRNÁ* ZMĚNĚ DIPOLOVÉHO MOMENTU BĚHEM VIBRAČNÍHO POHYBU**

Infračervená spektrometrie

TYPY VIBRACÍ

- VALENČNÍ – ZMĚNA délky vazby/vazeb

» SYMETRICKÁ

» ANTISYMETRICKÁ

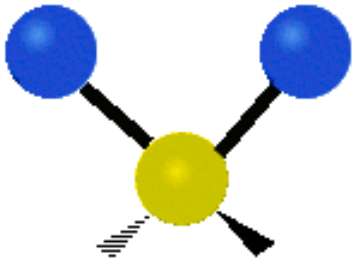

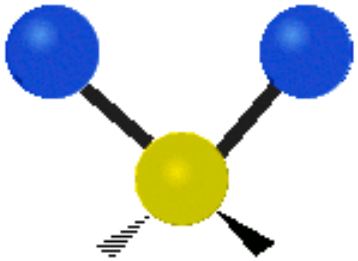

Infračervená spektrometrie

TYPY VIBRACÍ

- DEFORMAČNÍ - změny úhlů (vazebné úhly, torsní úhly)
- nůžková, kolébavá, kývavá, kroutivá

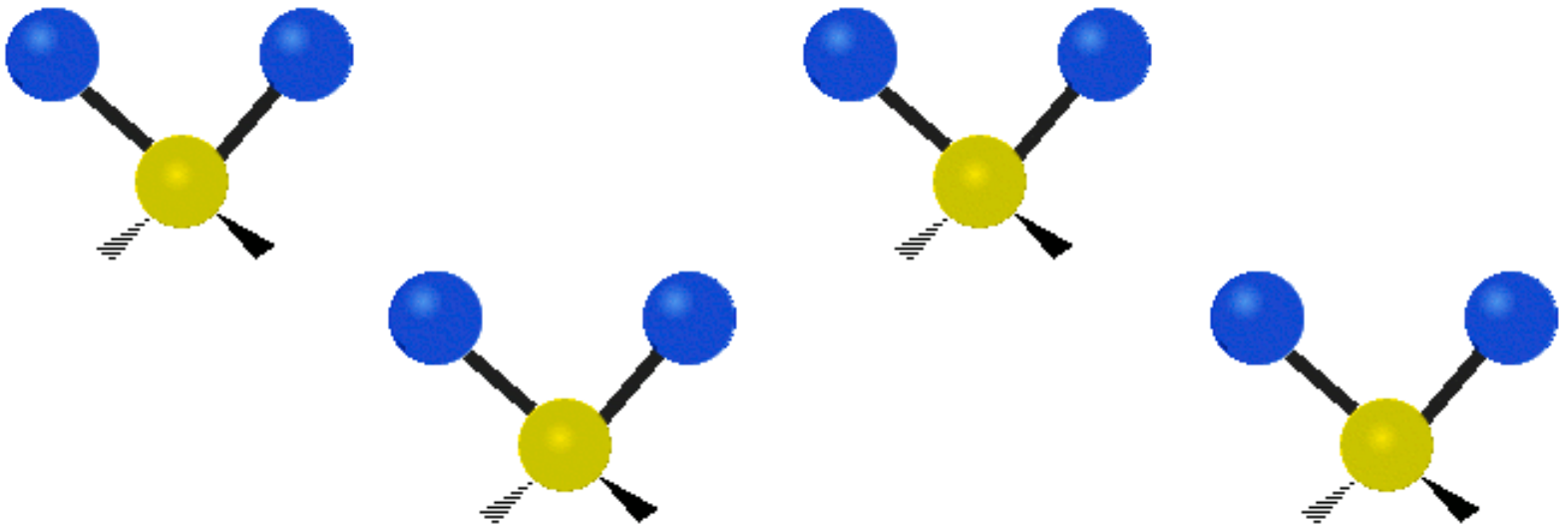

FT-IR reflexní techniky

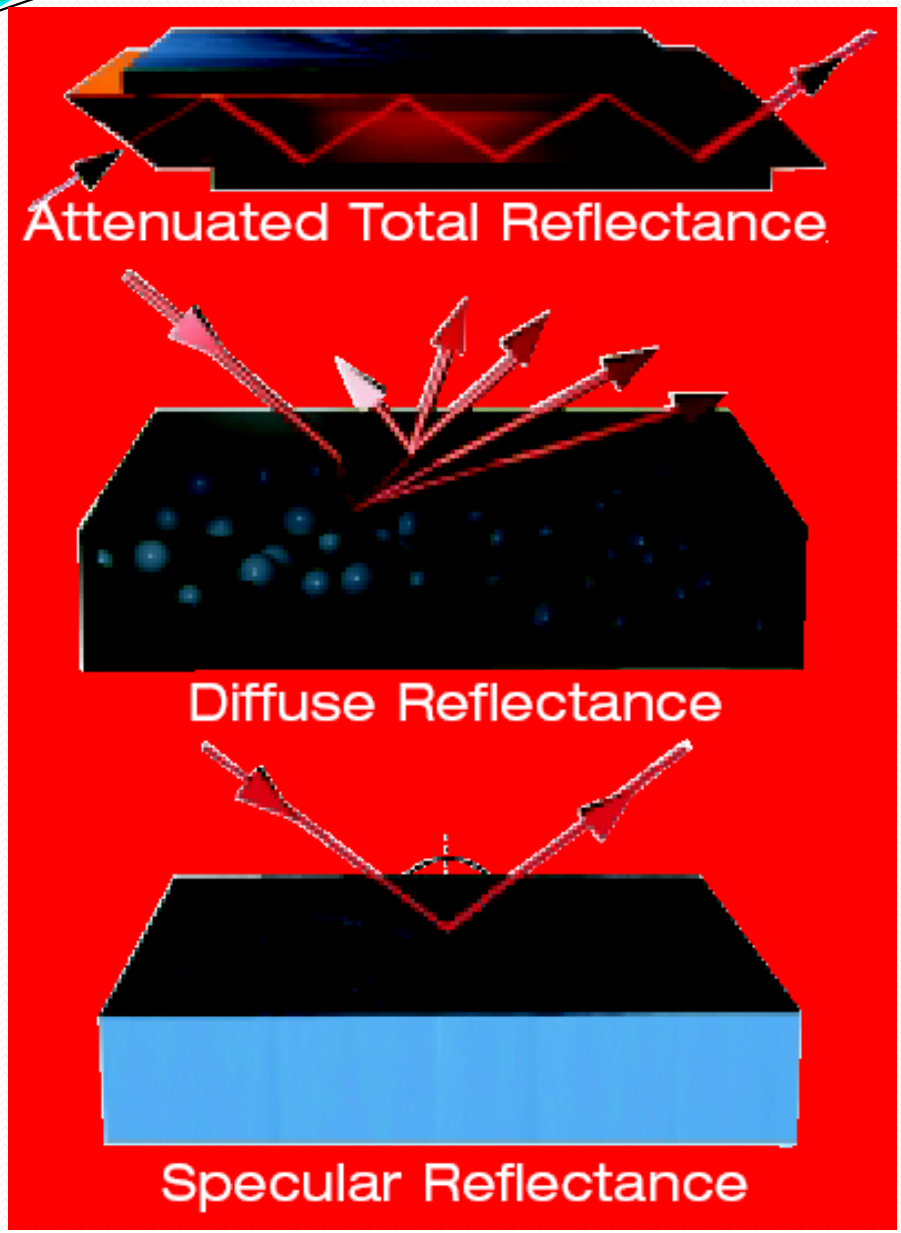

- Infračervený paprsek se odráží od fázového rozhraní úplným vnitřním odrazem
- Vzorek musí být v optickém kontaktu s krystalem
- Snímaná informace z **povrchové vrstvy** vzorku

- Pevné látky – prášková forma , případně naředěná IČ transparentní matricí - (KBr)
- Informace **z objemu vzorku**

- Reflektující vzorek či spíš tenká vrstva na zrcadlovém podkladu
- Informace **z tenké (povrchové) vrstvy**

Infračervená spektrometrie

- **Reflexní techniky**

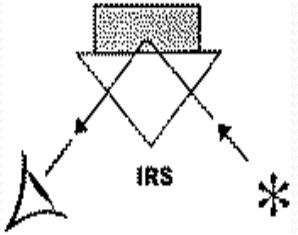

ATR - attenuated total reflection

- zeslabený úplný (vnitřní) odraz

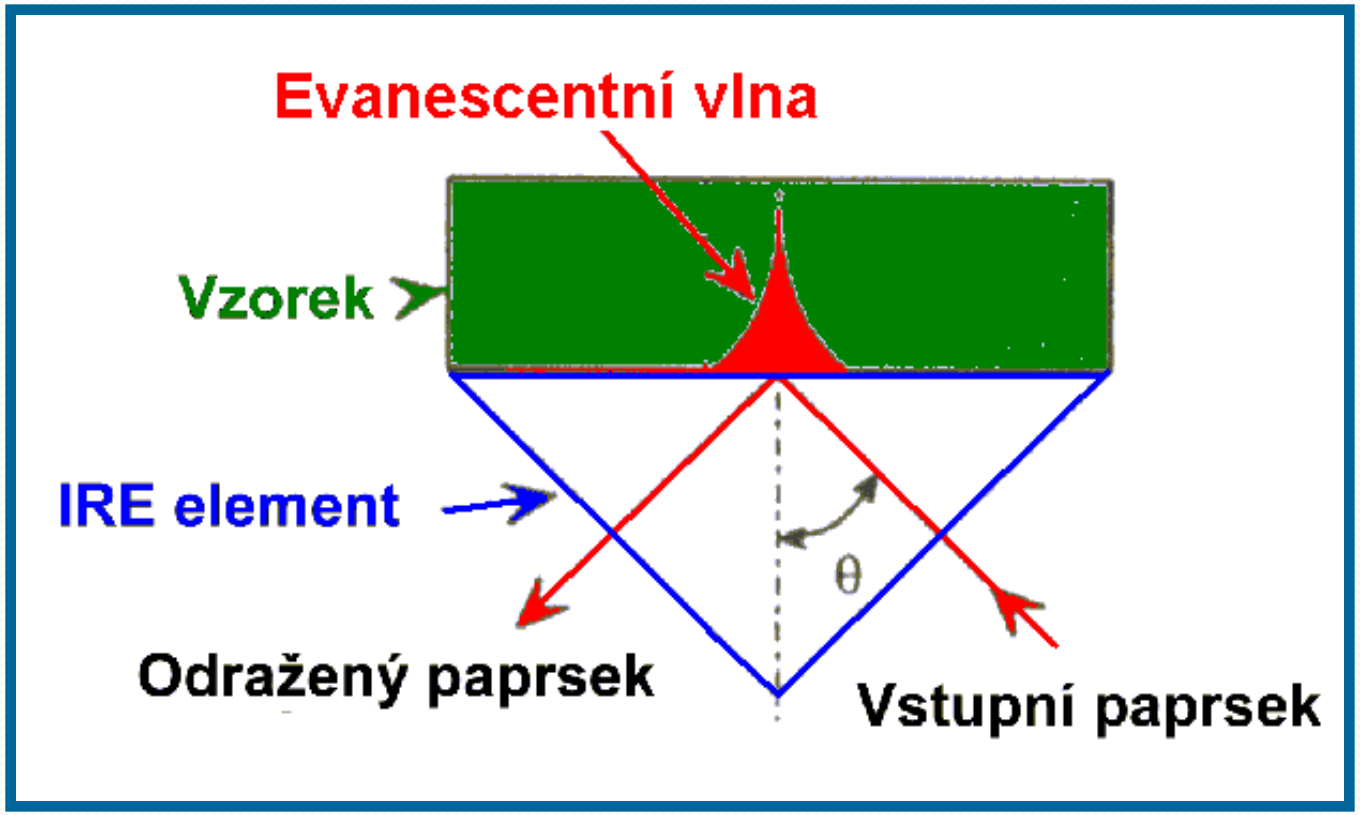

Infračervená spektrometrie

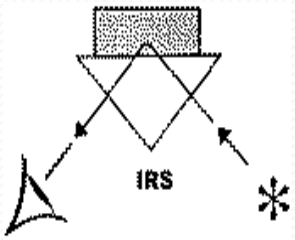

- Faktory, které ovlivňují ATR spektrální analýzu

POUZE ODRAZ - NIKOLI LOM !

- Vlnová délka infračerveného záření
- Index lomu IRE a vzorku
- Hloubka průniku
- Efektivní délka dráhy
- Úhel dopadu
- Účinnost kontaktu se vzorkem
- Materiál IRE (ATR krystalu)

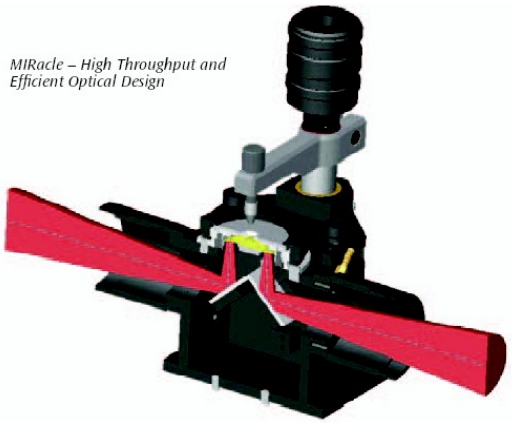

Zeslabený totální odraz (ATR)

Chart of Common Crystal Materials

Material	ATR Spectral Range (cm^{-1})	Refractive Index	Depth of Penetration (μ) (at 45° & 1000 cm^{-1})	Uses
Germanium	5,500 - 675	4	0.66	Good for most samples. Strong absorbing samples, such as dark polymers.
Silicon	8,900 - 1,500 & 360-120	3.4	0.85	Resistant to basic solutions.
AMTIR	11,000 - 725	2.5	1.77	Very resistant to acidic solutions.
ZnSe	15,000 - 650	2.4	2.01	General use.
Diamond	25,000 - 100	2.4	2.01	Good for most samples. Extremely caustic or hard samples.

Infračervená spektrometrie

ATR - instrumentace

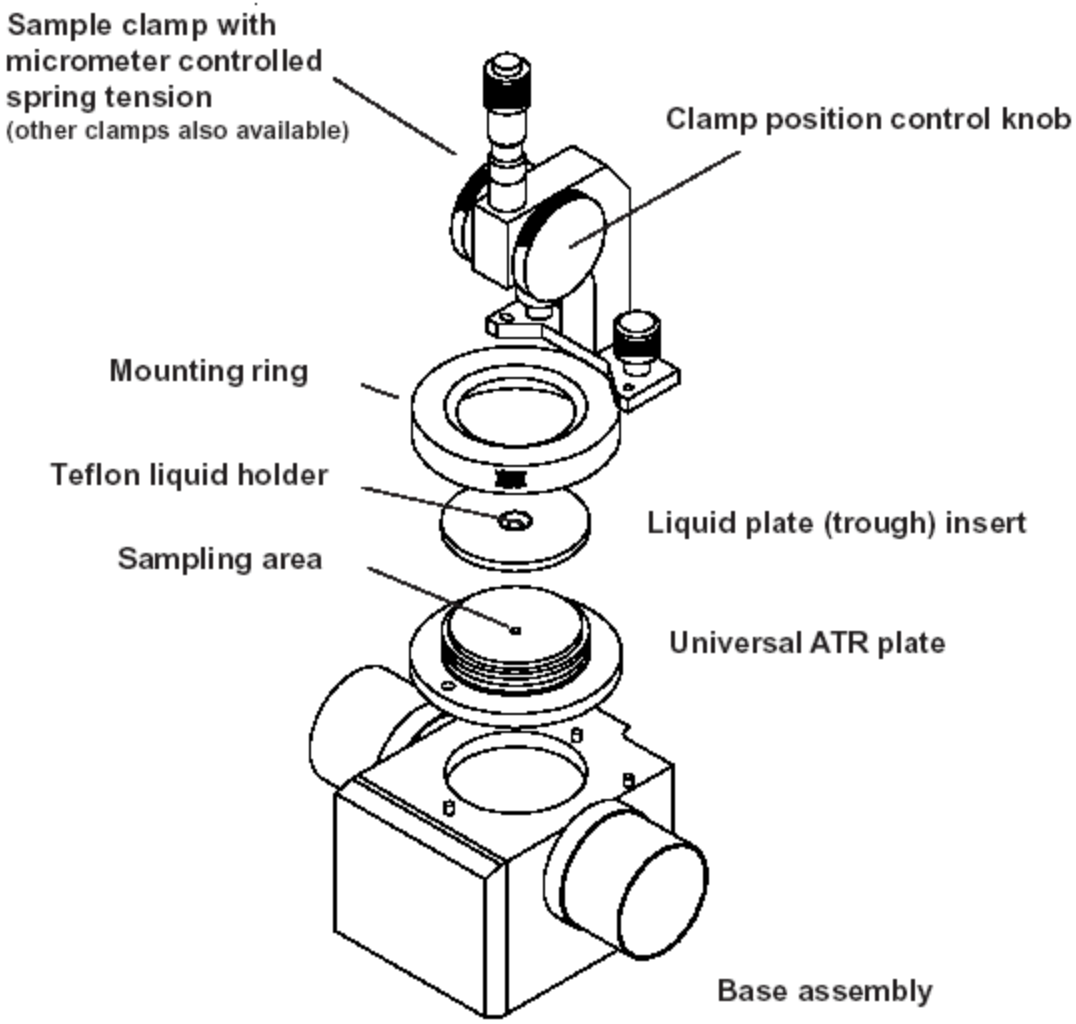

Single Reflection ATR Plate

3 Reflection ATR Plate
(includes 5mm swivel tip)

ATR - instrumentace

MIRacle Pressure Clamps are Pinned-in-Place and Easily Upgraded

MIRacle Digital Clamp *Ideal for Controlled Pressure*

MIRacle Rotating Clamp *Ideal for Cleaning Tip of Debris*

MIRacle Viewing Clamp *Ideal for Placing Fibers or Crystals*

MIRacle High-Pressure Clamp *– Ideal for Routine Sampling*

MIRacle Micrometer Clamp *– OK for Low Pressure Applications*

Slide 12

Sample should completely cover the ZnSe Crystal indicated with the arrow below.

Slide 13

Be sure that the press is rotated completely to the lowest level.

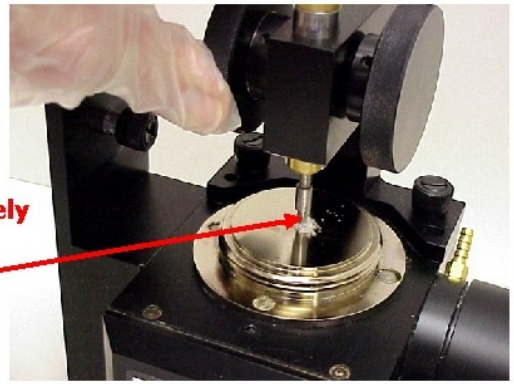

ATR - instrumentace

Zeslabený totální odraz (ATR)

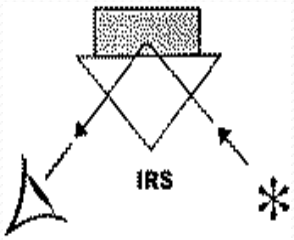

Scheme of the Circle ATR Cell

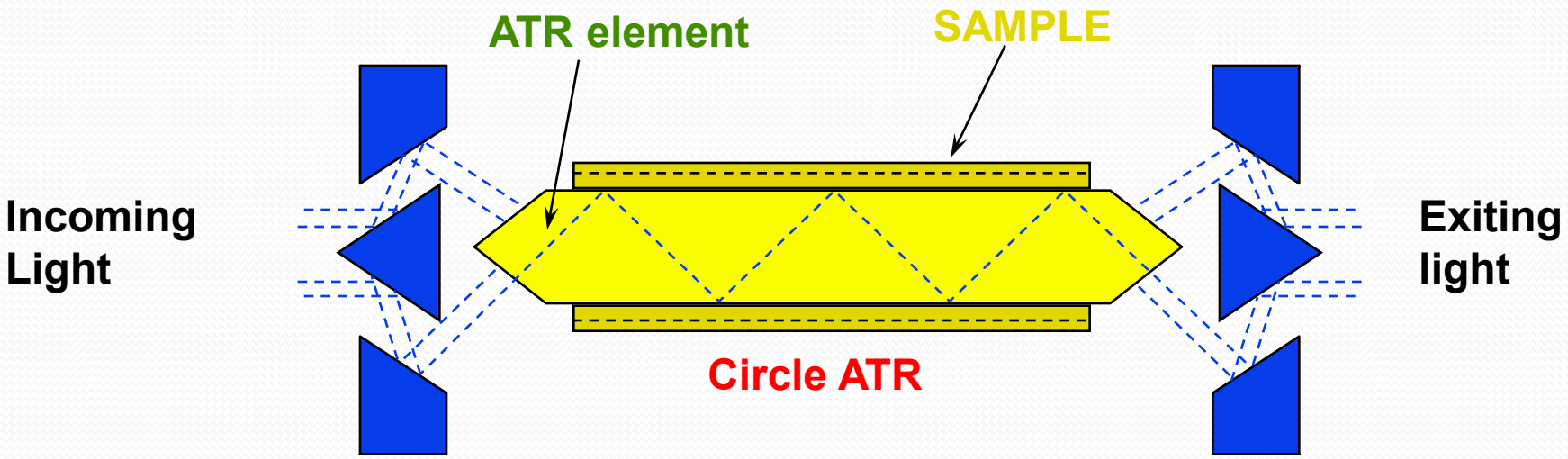

Attenuated Total Reflection (ATR)

ATR Spectra – Ge crystal

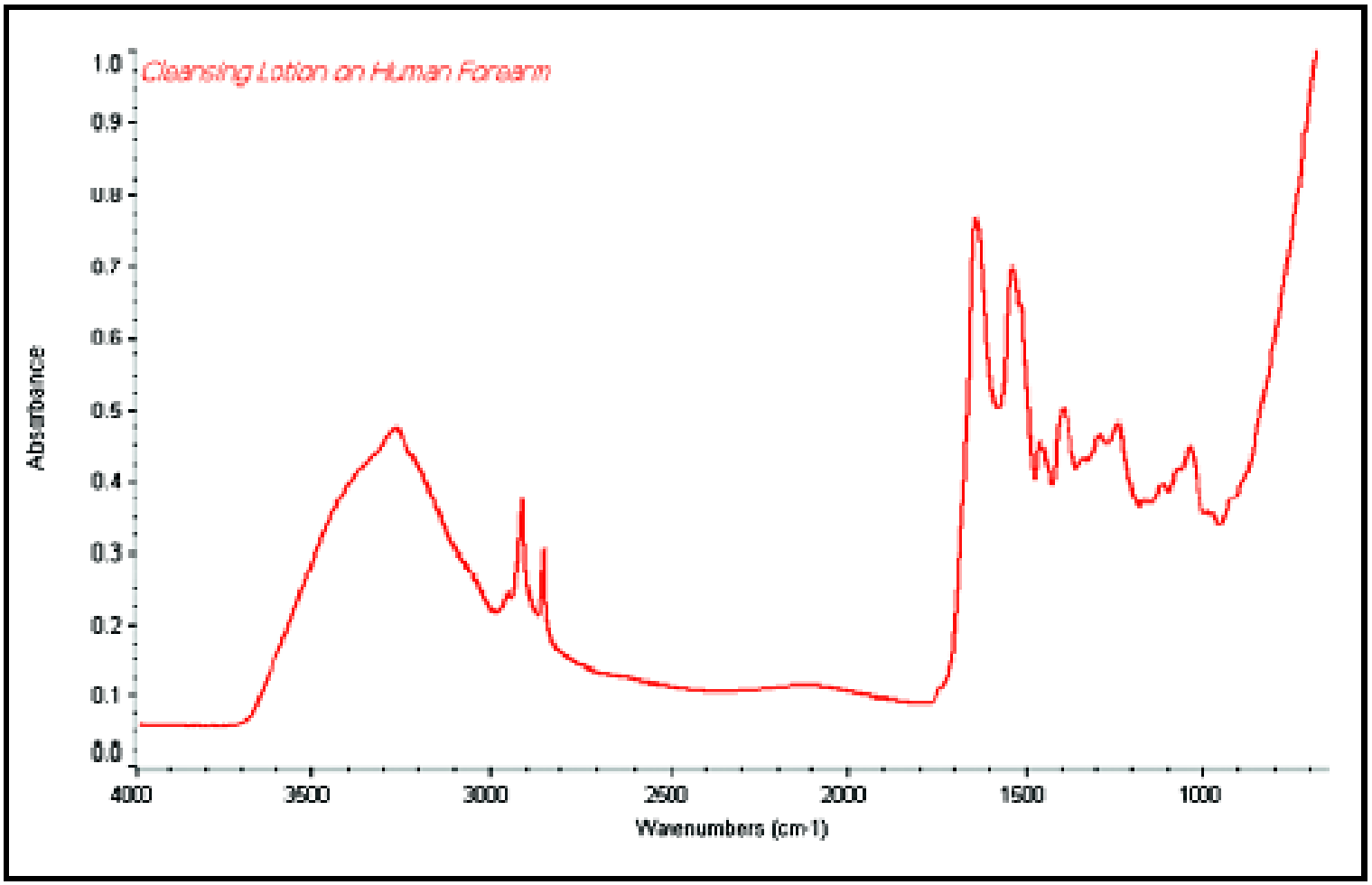

FTIR spectrum of cleansing lotion on human forearm – using the HATRPlus with flat plate Ge crystal.

Attenuated Total Reflection (ATR)

ATR Spectra of Rubber – Diamond vs Germanium IRE

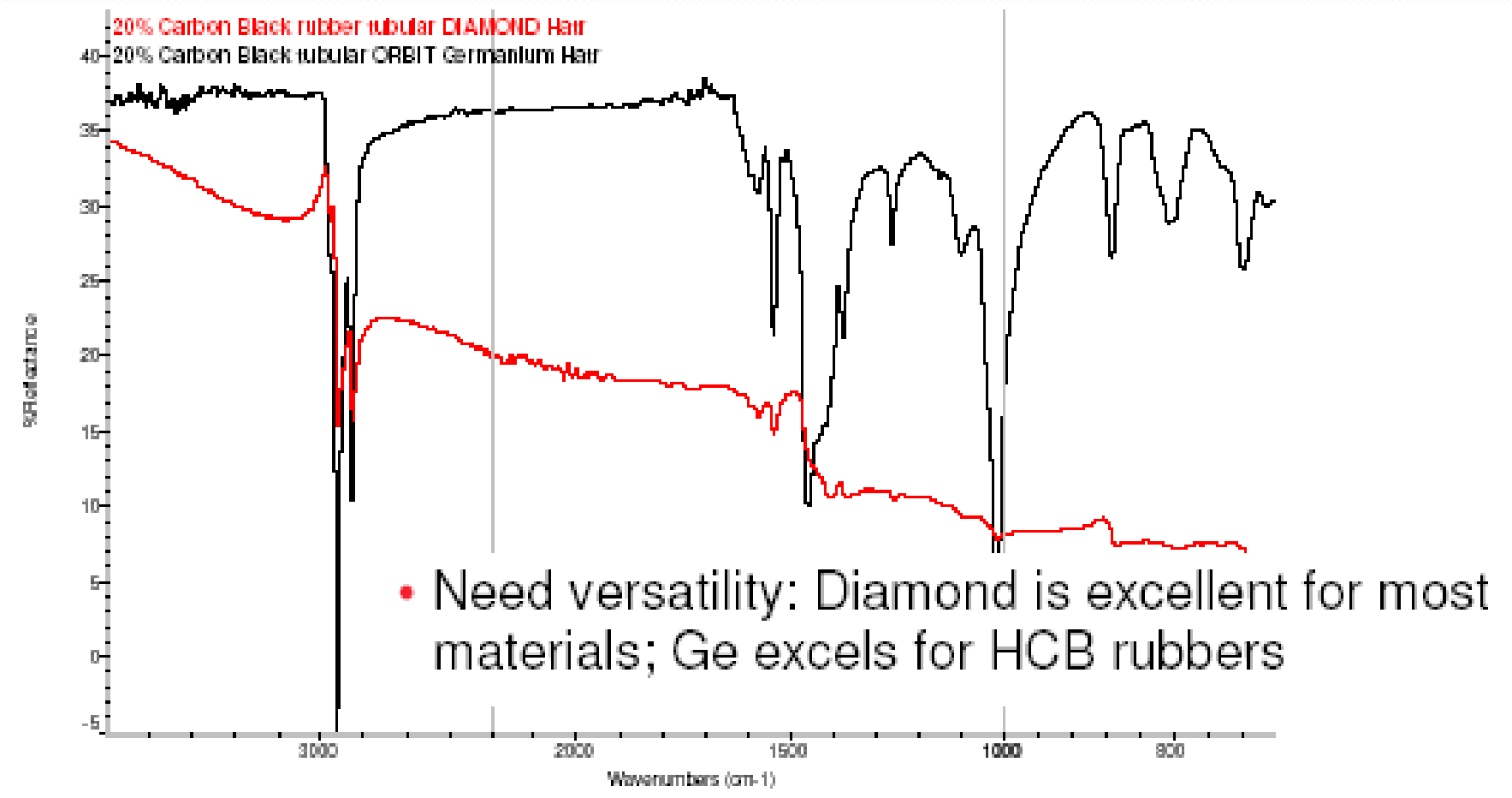

Refractive indexes: Ge=4

Diamond=2.4

Spekulární vs. Difusní Reflexe

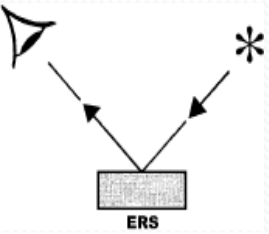

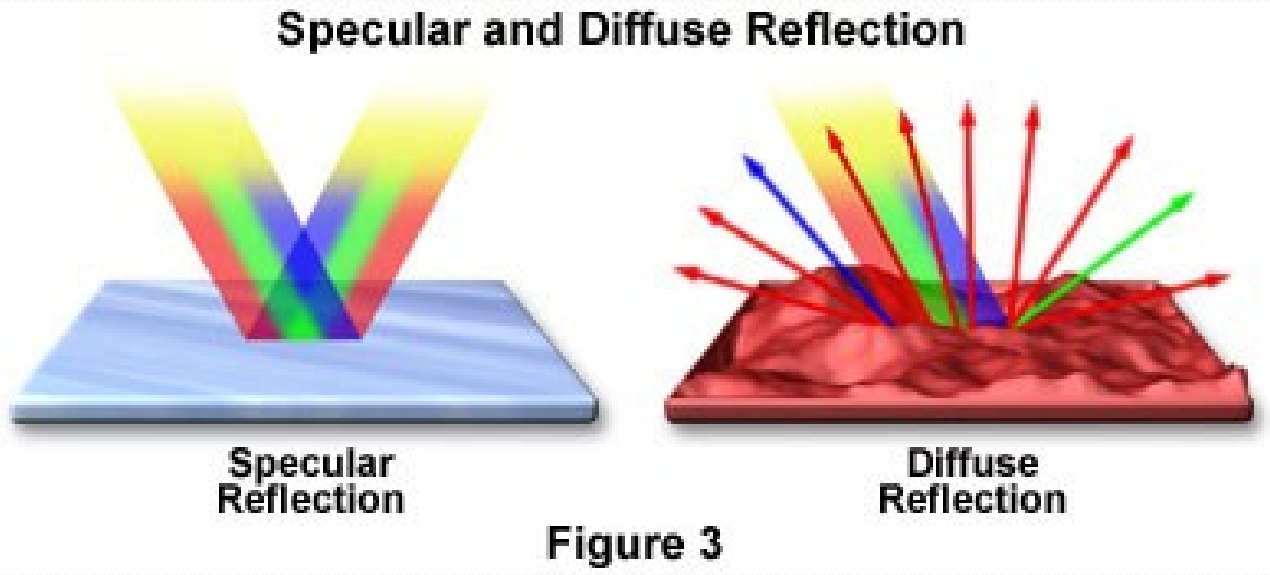

Figure 3

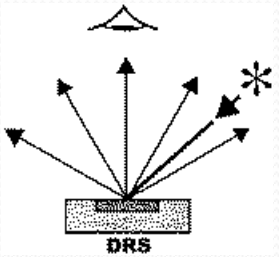

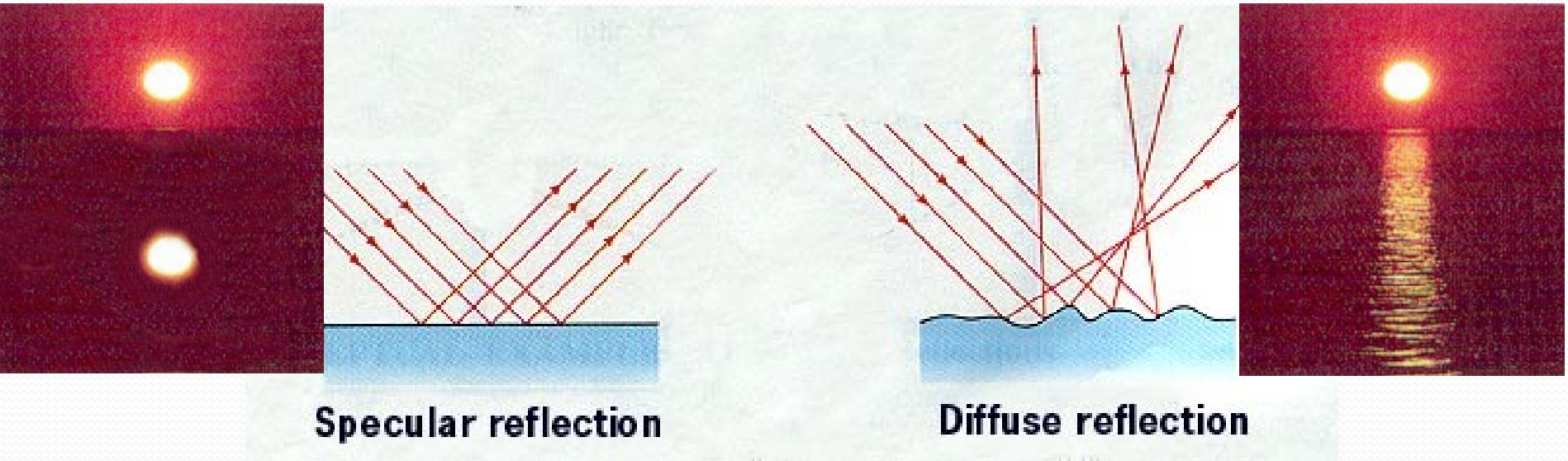

Reflexní techniky

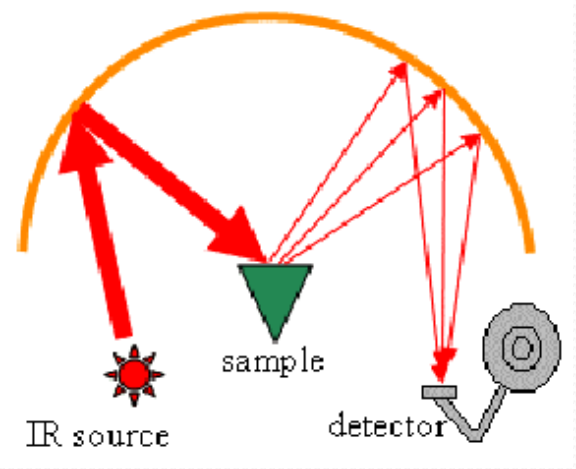

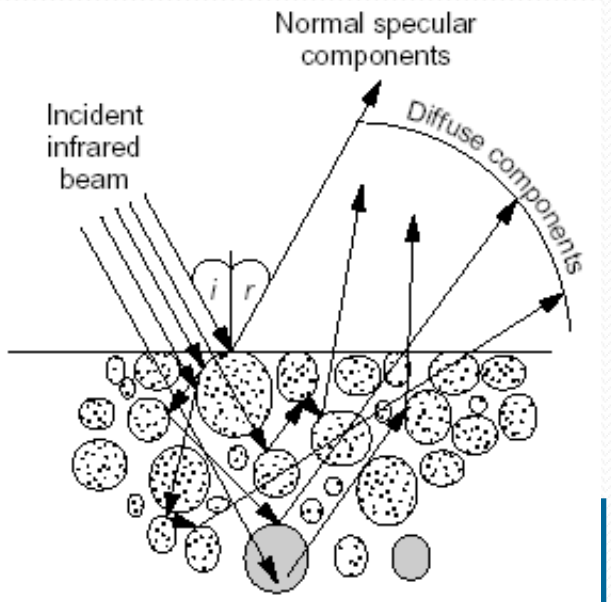

-DRIFT

-rychlé měření práškových vzorků

-- nízká opakovatelnost dat

- složitý fyzikální popis jevu

tvar částic, „zhutnění“ vzorku

index lomu částic

reflektivita a absorpční vlastnosti částic

Diffuse Reflection

Experimental Setup

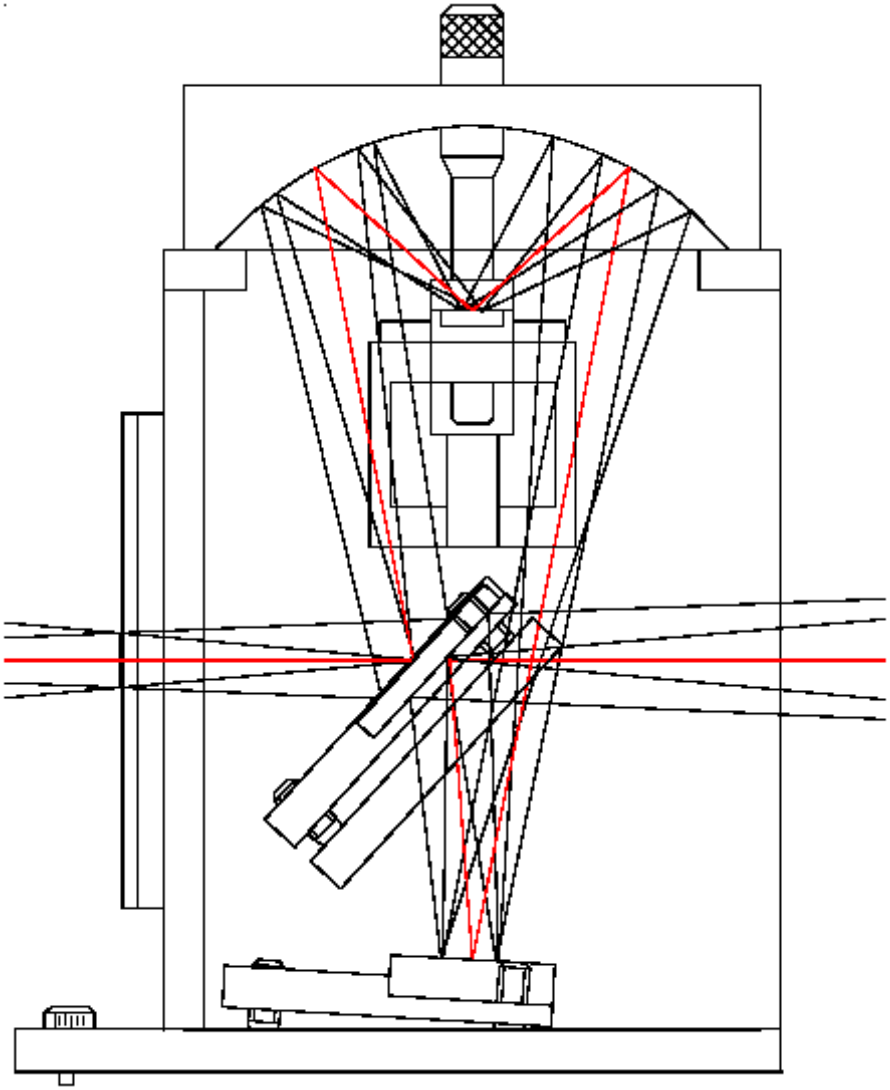

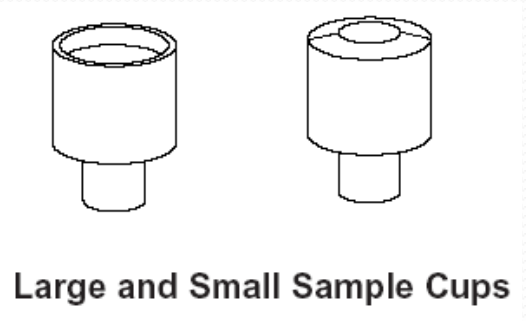

Large and Small Sample Cups

Diffuse Reflection

Experimental Setup – Different Geometry

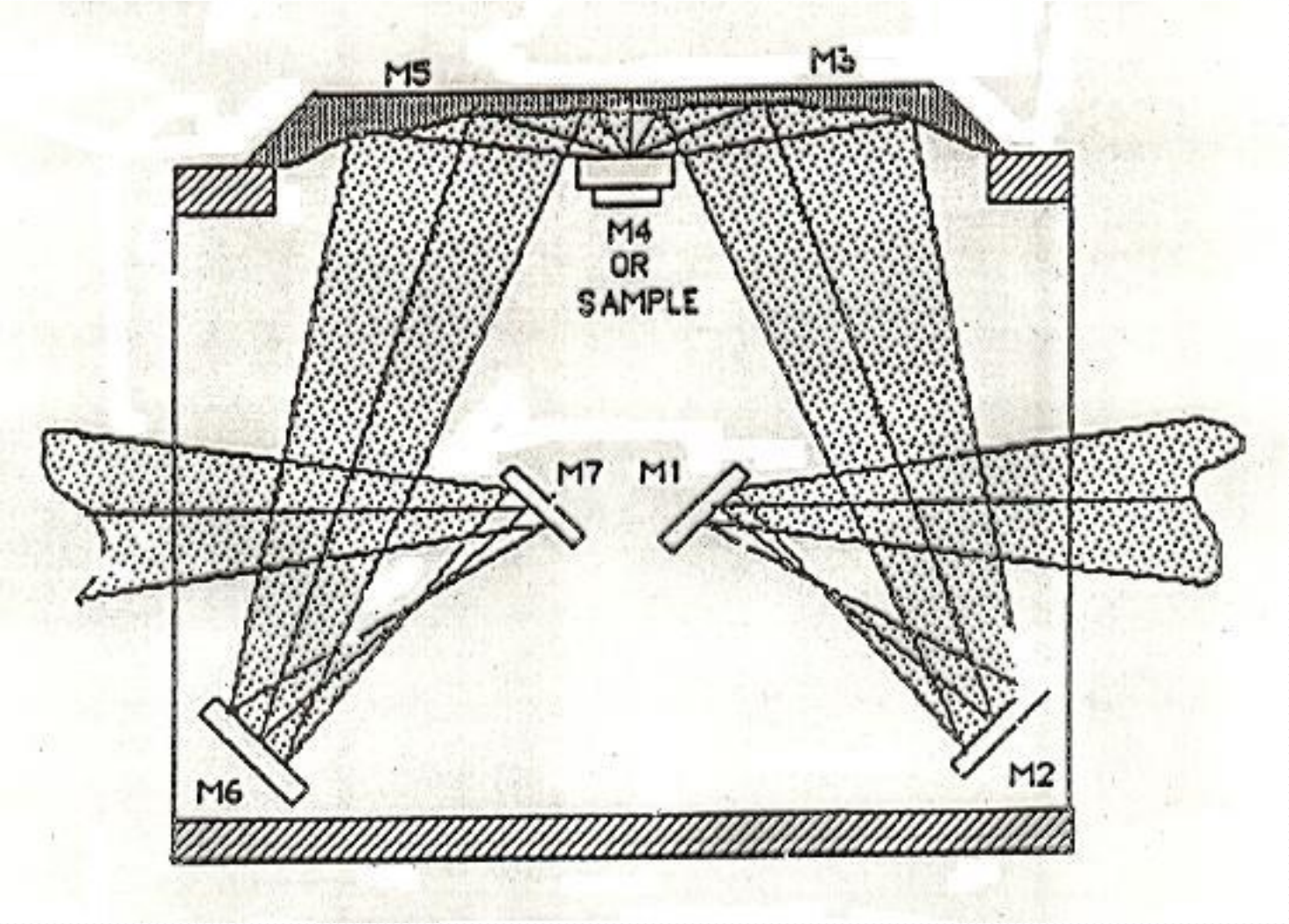

Diffuse Reflection

IR Spectra of $CaCO_3$

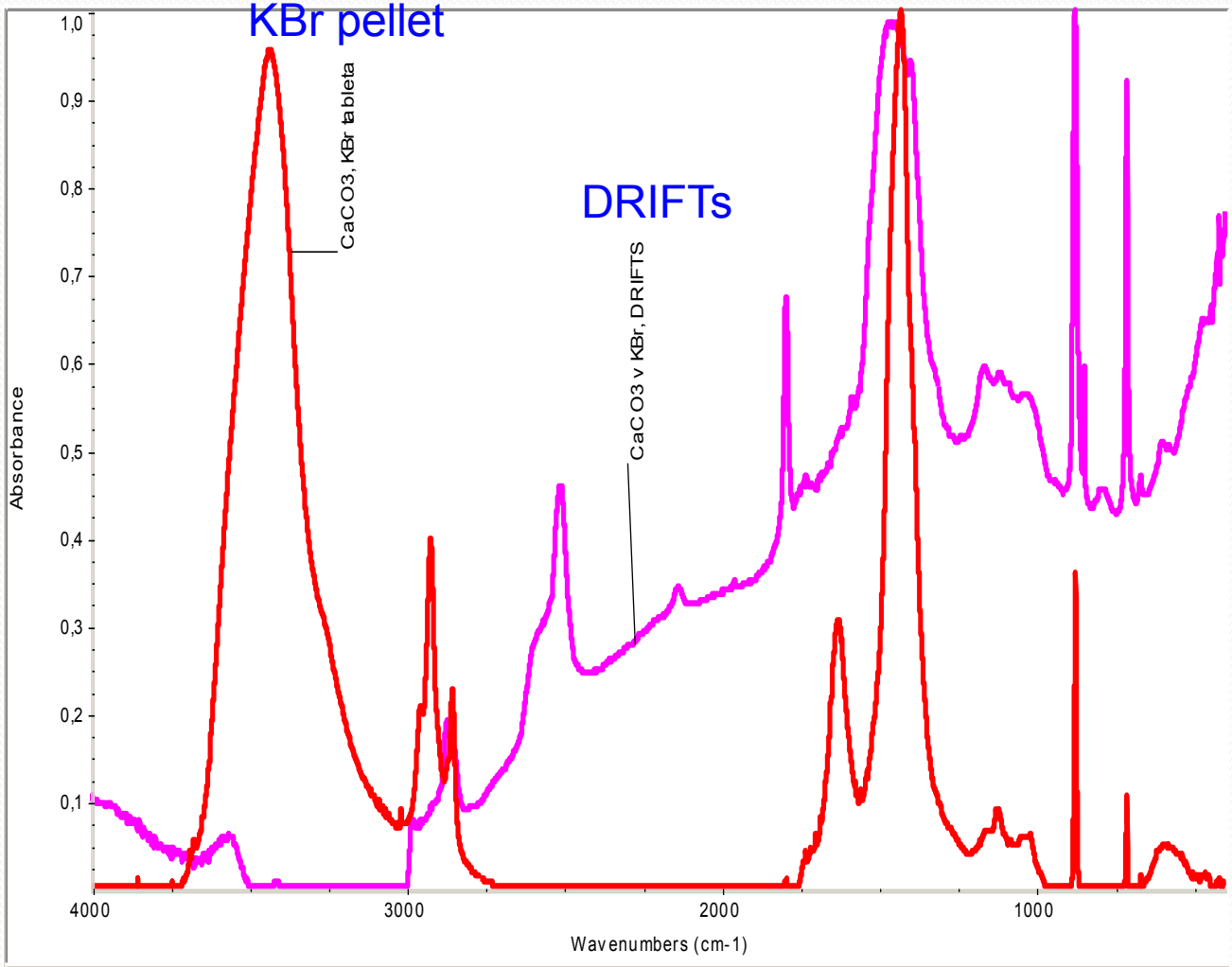

Diffuse Reflection

IR Spectra of 1,2-Bis(diphenyl phosphino)ethane

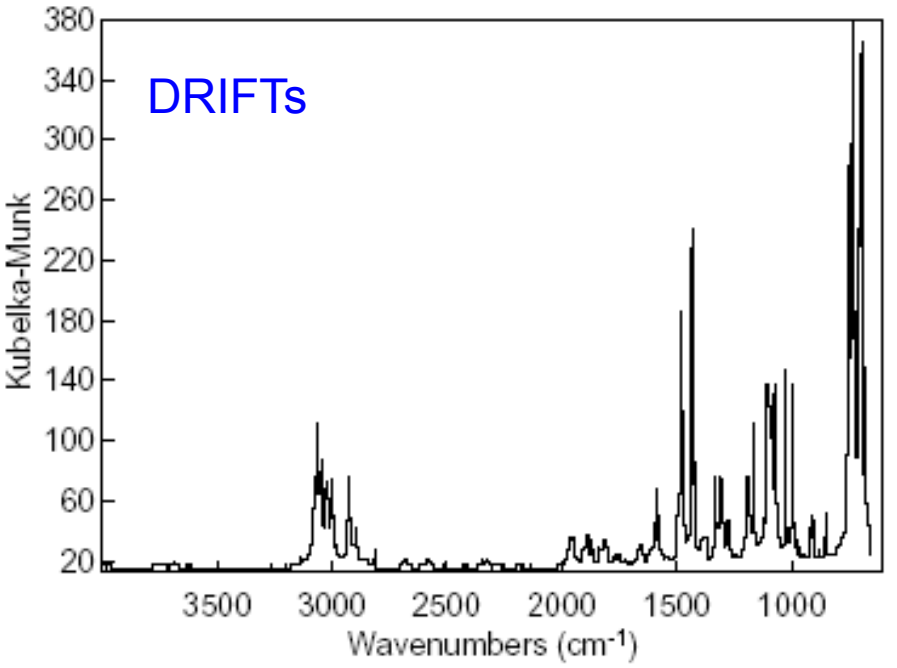

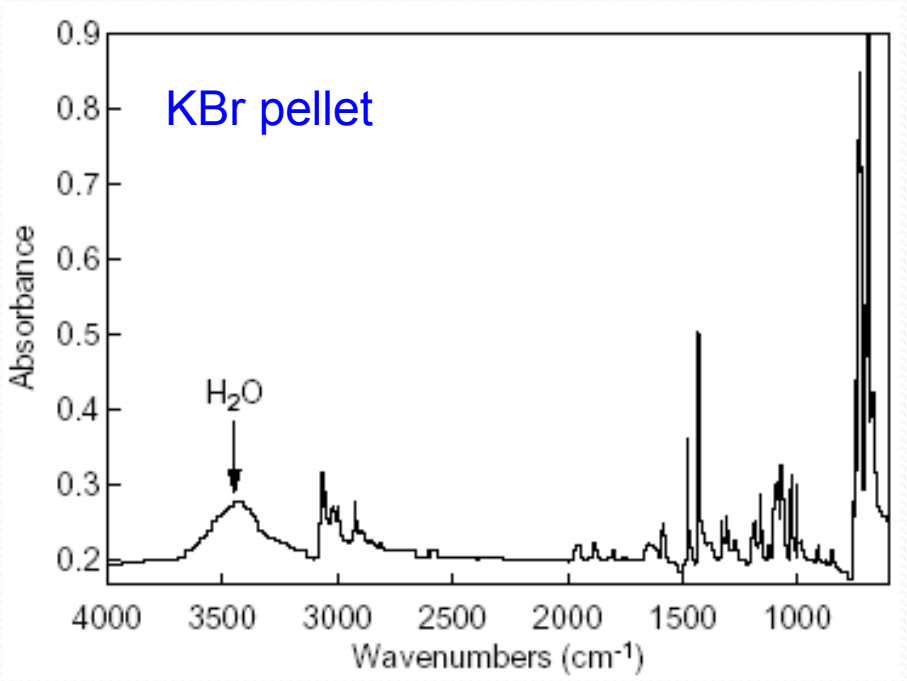

T Armaroli et al. Oil & Gas Science and Technology – Rev. IFP, 59 (2004), 215.

Specular Reflection

If the surface is smooth like a mirror:

– reflection and the incidence angles are equal

– reflected beam retains the polarization characteristics of the incidence beam

Thin layers: 0.5-20 mm $\Rightarrow$ angle ~20-60^{o} $\Rightarrow$ spectra similar to transmission ones

Monomolecular layers: angle ~60-85^{o} $\Rightarrow$ spectra predominatly a function of the **refractive index**

$\Rightarrow$ derivative shape of the bands arising from superposition of extinction coefficient and dispersion of refractive index

Specular Reflection

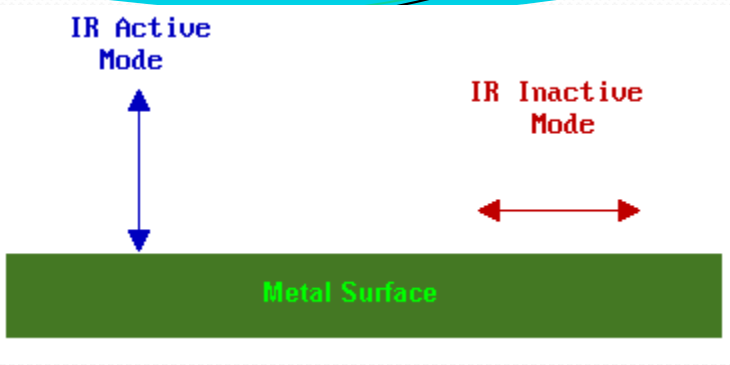

Experimental Setup

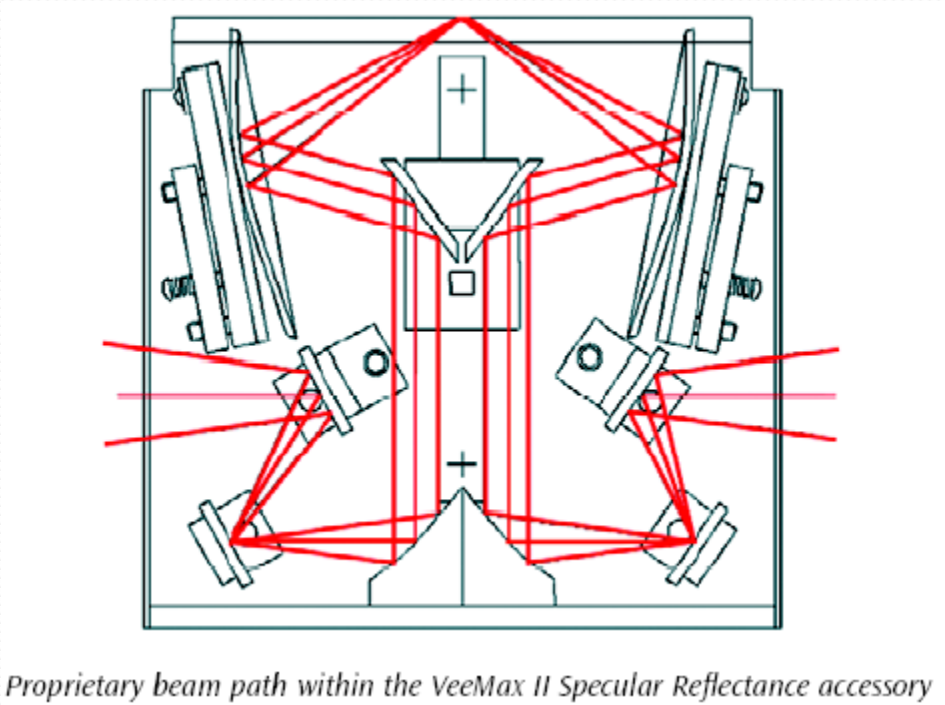

Proprietary beam path within the VeeMax II Specular Reflectance accessory

- **selection of incident angle**

Incident angle influences
- effective pathlength
- **polarized IR response**

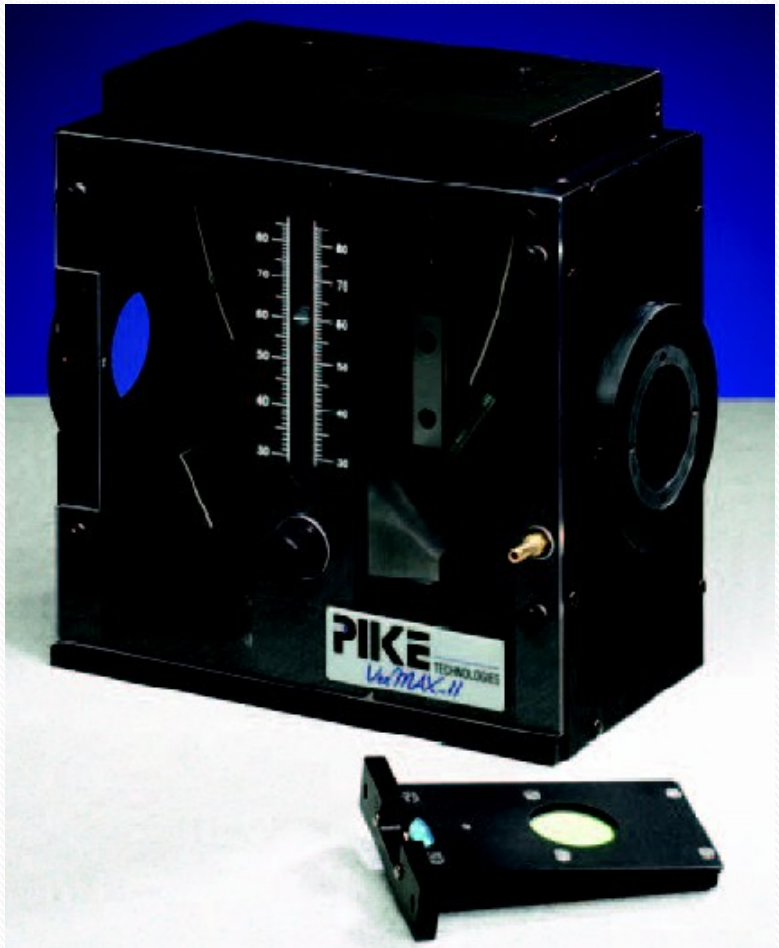

Specular Reflection

Refractive index

Absorbance index

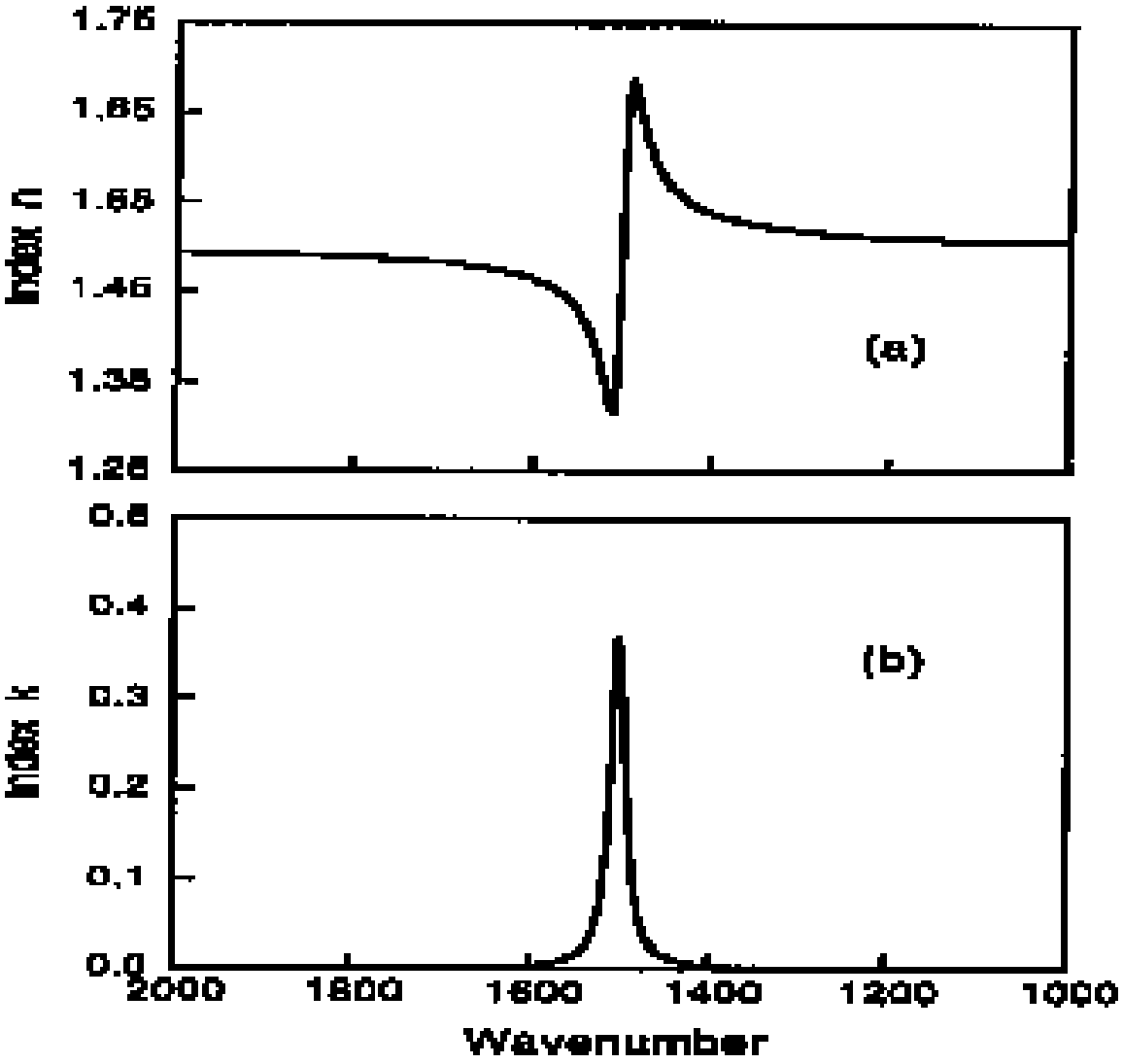

K. Yamamoto and H. Ishida, Vibrational Spectrosc., 8, 1 (1994)

Specular Reflection

Correction of „Restrahlen „ bands

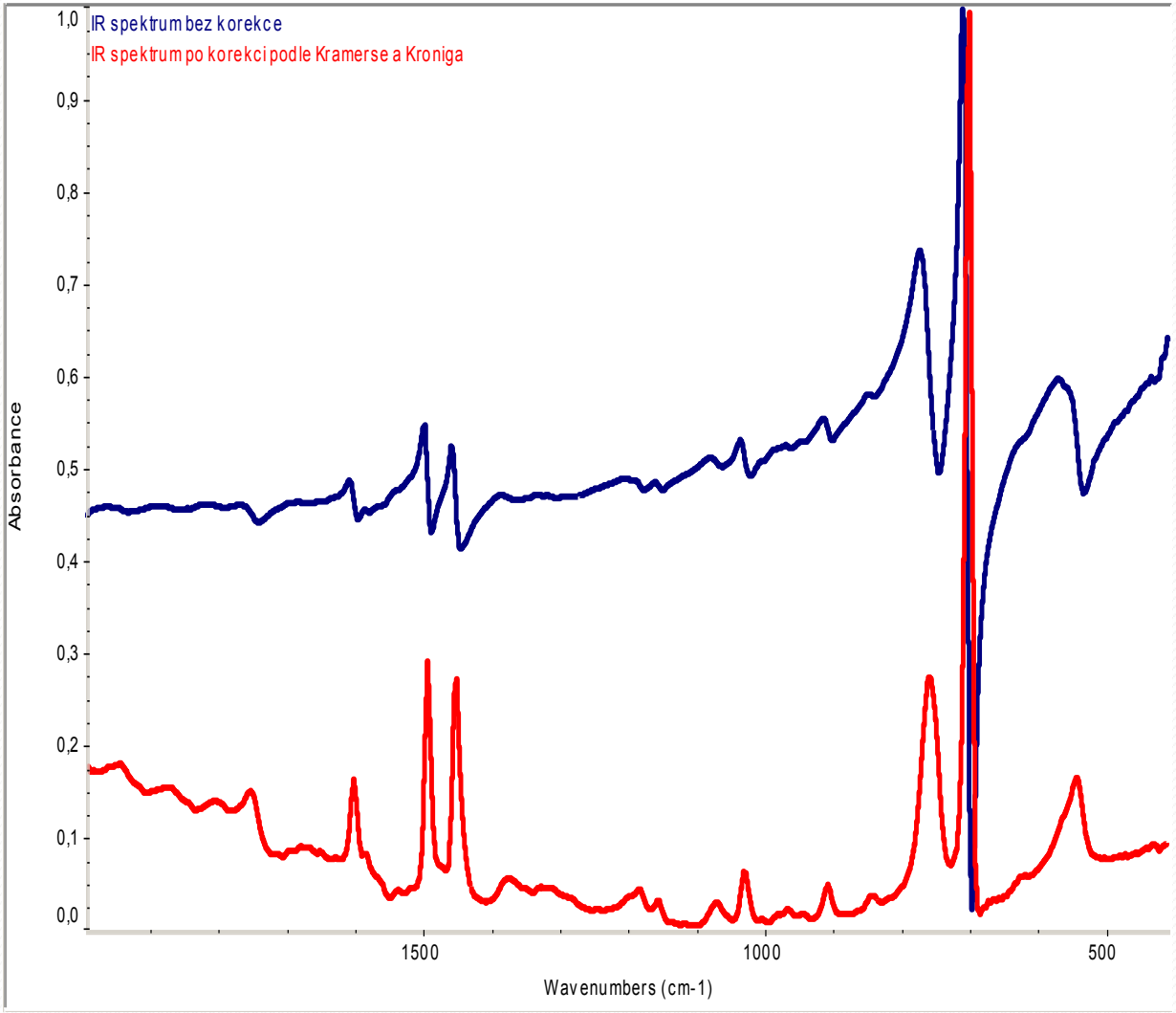

Specular Reflection

Correction Kramers-Kronig

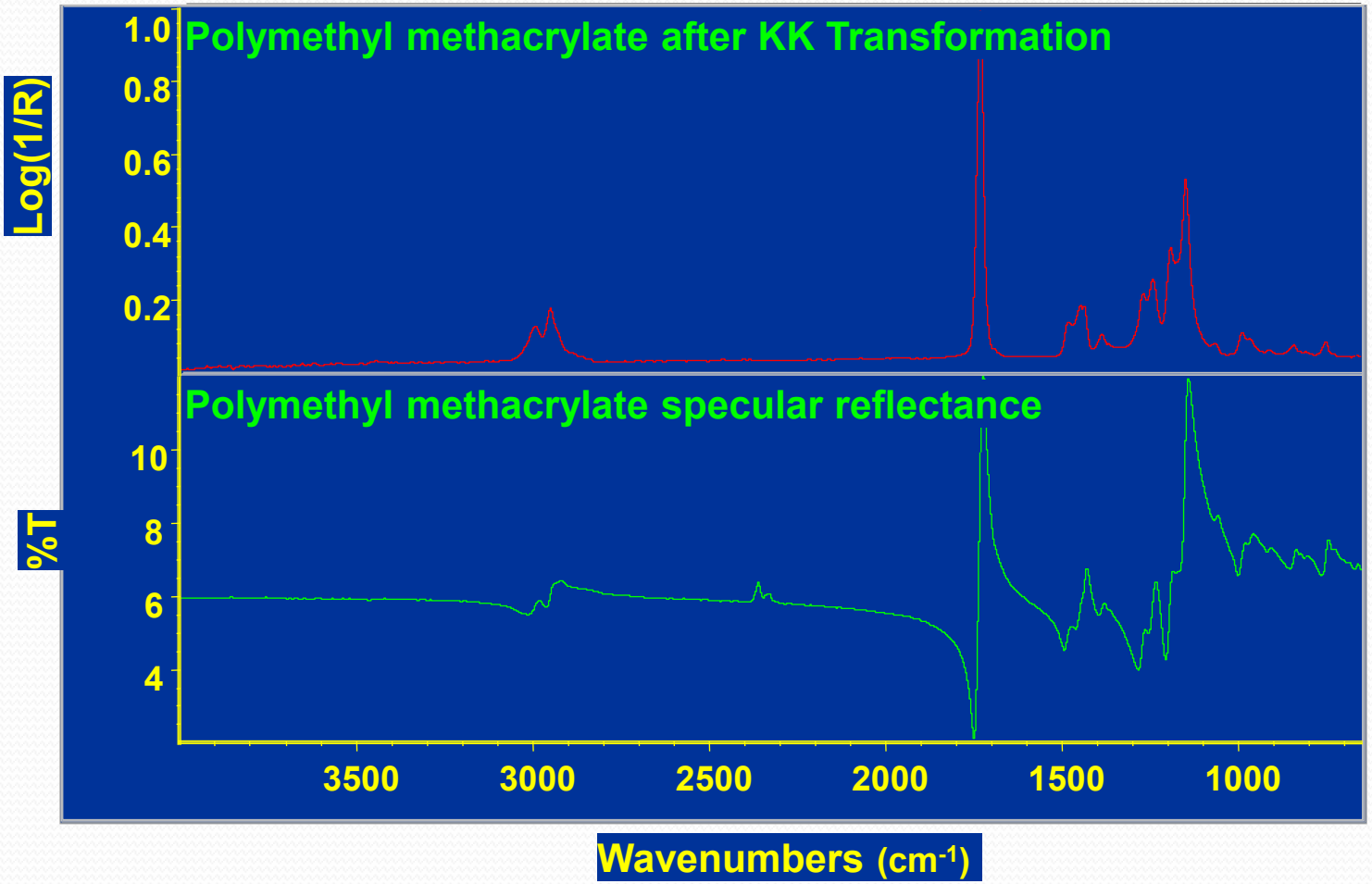

Nanospectroscopy and microspectroscopy

- Chemical images of samples
  - Generate from peak heights, areas, peak ratios, correlation, results of principal component analysis etc.
  - Useful for monitoring changes in chemical composition in a sample
    - inhomogeneities, defects, composite materials …

Nanospectroscopy and microspectroscopy

- Chemical images of sample
  - Group of points collected over the entire area of interest
  - Points can be collected in series (mapping – scanning the surface) or in parallel (imaging – multichannel detection)

Area Mapping and Imaging

- Group of points collected over the entire area of interest
- Points can be collected in series (mapping) or in parallel (imaging)
- Ideal for analysis of highly heterogeneous samples

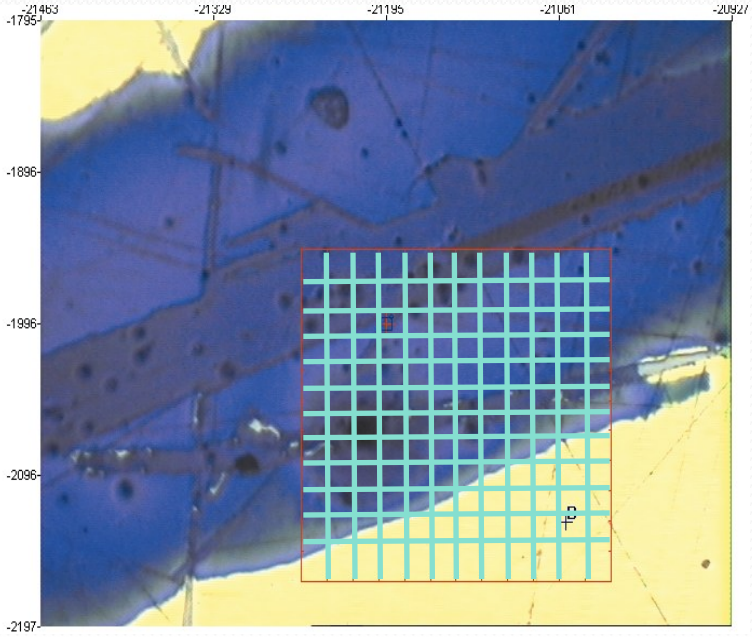

- **Chemical images of sample**
  - **IR imaging – multichannel detection**

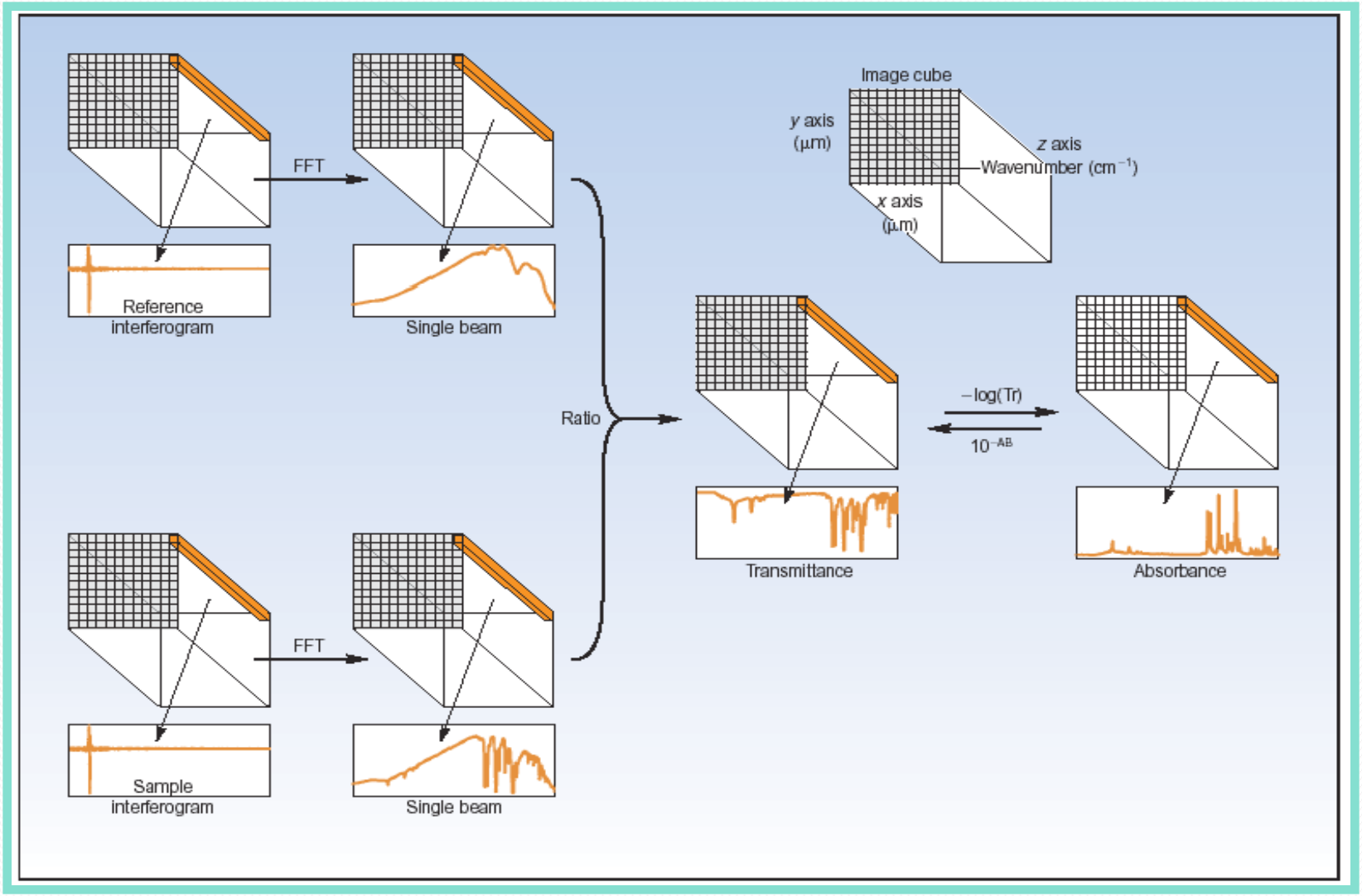

- **Chemical images of sample**
  - **IR imaging – multichannel detection**

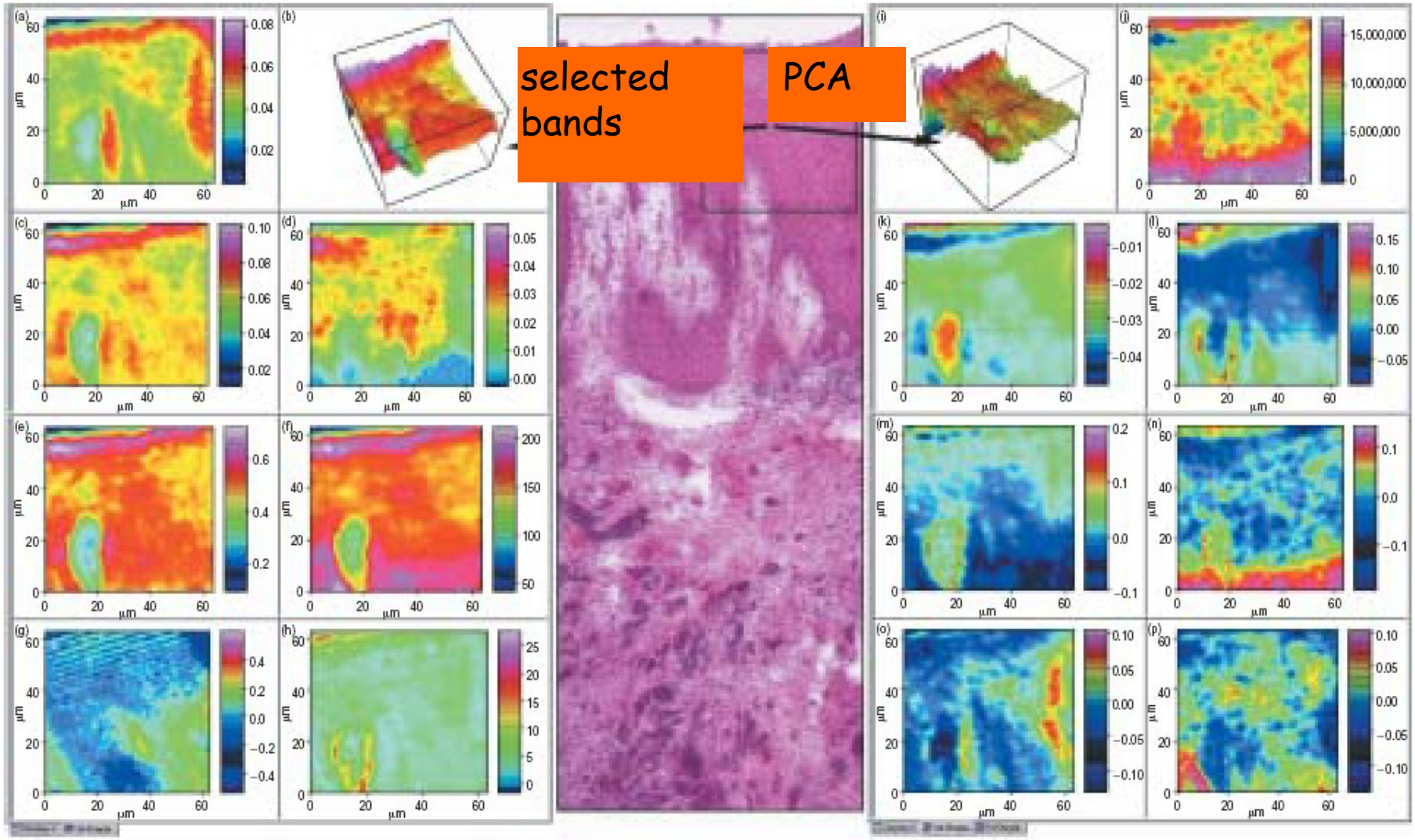

Nanospectroscopy vs. microspectroscopy

- Microspectroscopy – techniques of far field
- Nanospectroscopy – techniques of near field
  - "coupling of a probe and surface"

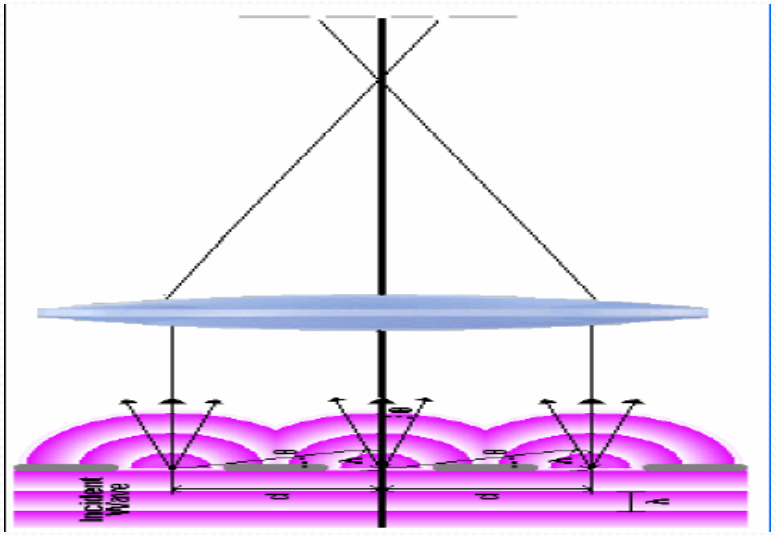

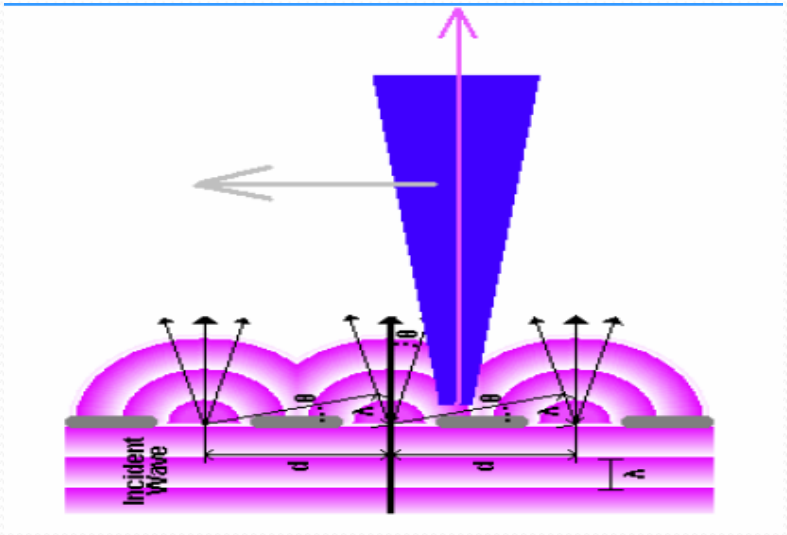

Nanospectroscopy vs. microspectroscopy

- Microspectroscopy – techniques of far field
  - The maximum spatial resolution in a properly designed microscope is limited by the **diffraction** of light.
- Nanospectroscopy – techniques of near field
  - The maximum spatial resolution is under diffraction limit, it is limited mostly by probe aperture (probe diameter).

Microspectroscopy

Spatial Resolution

- the ability to view two closely spaced points as distinct objects

Diffraction

- the bending (or "scattering") of light/energy by an opening of an optical element (lens, aperture)

Microspectroscopy

Diffraction

- the bending of light by an opening of an optical element
- occurs when the wavelength of the light approaches the size of the opening
- for infrared spectroscopy ~ 10 μm
  - (1000 cm^{-1} is 10 μm)
- for Raman spectroscopy better than 1 μm
  - excitation in visible range

Microspectroscopy

Diffraction

$$d = \frac{1.22\ \lambda}{\text{NA obj.} + \text{NA cond.}}$$

For 1469 cm^{-1},

(1469 cm^{-1} = 6.8 μm)

$$d = \frac{1.22\ (6.8\ \mu m)}{0.58 + 0.71} = 6.4\ \mu m$$

Microspectroscopy

Diffraction, resolution, sample size

Large sample (>100 μm)
No apparent diffraction

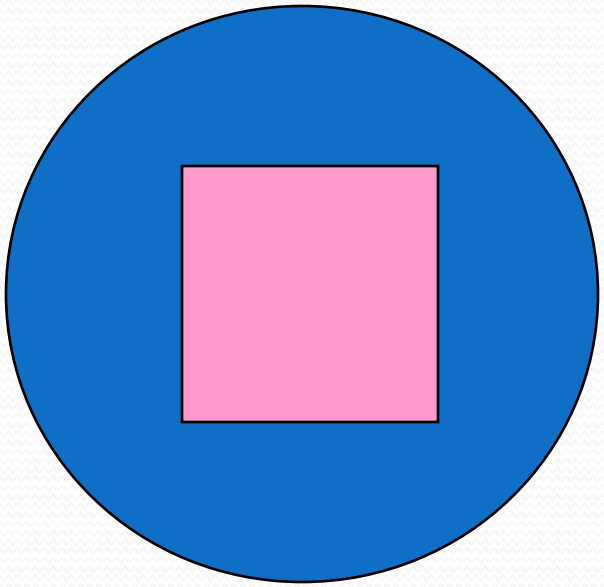

full field

sample area

Small sample (<100 μm)
Diffraction Present

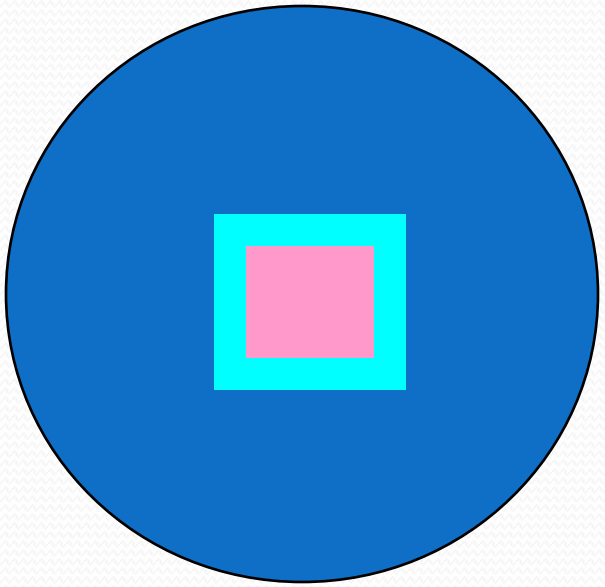

Diffracted radiation

Microspectroscopy

Minimize Diffraction Effect - Dual Remote Aperture

- First aperture placed between infrared source and sample, limiting IR beam to desired sample area
- Second aperture placed between sample and detector to reduce amount of diffracted light detected

Minimize Diffraction Effect - Dual Remote Aperture

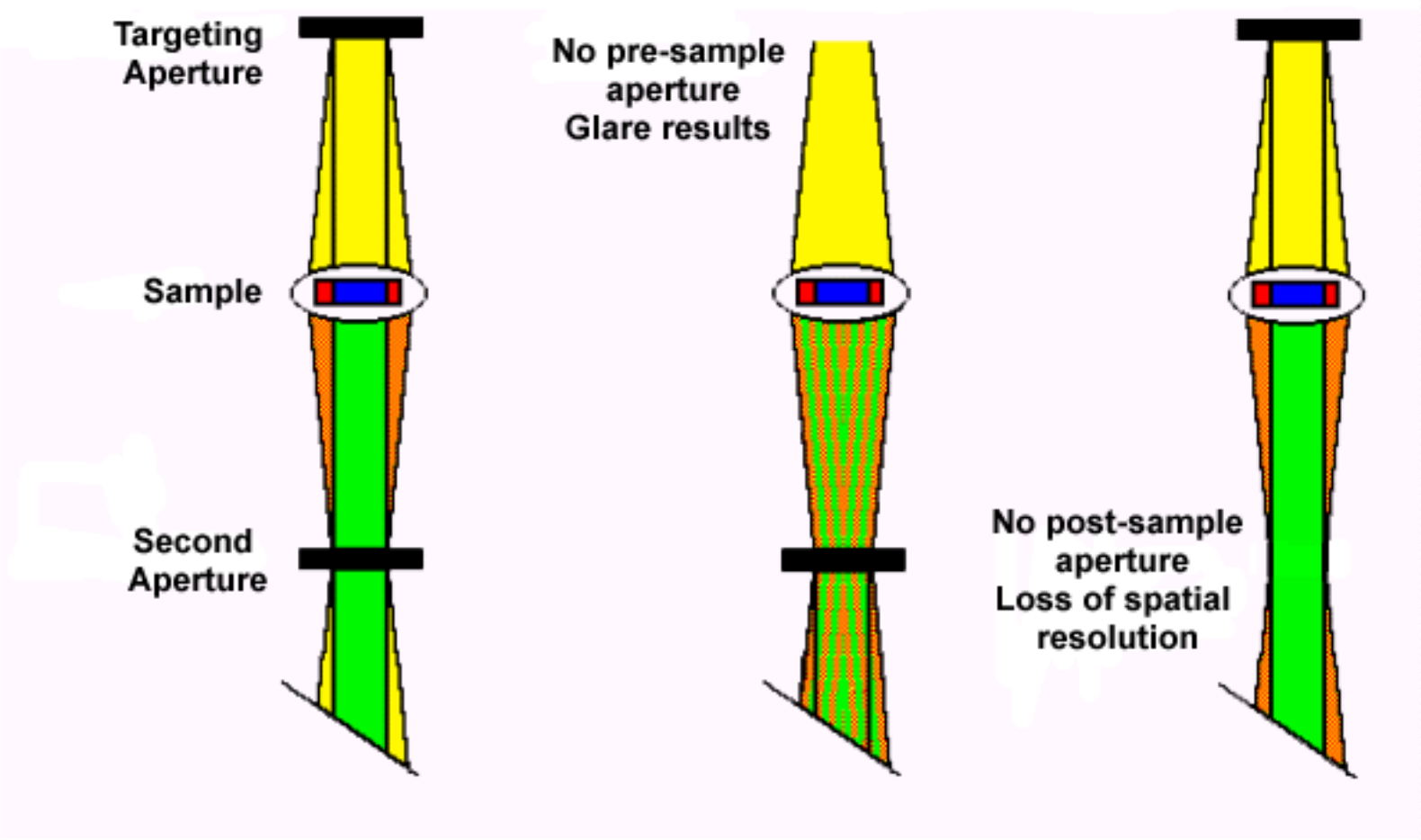

IR Microspectroscopy Sampling Modes

Transmission

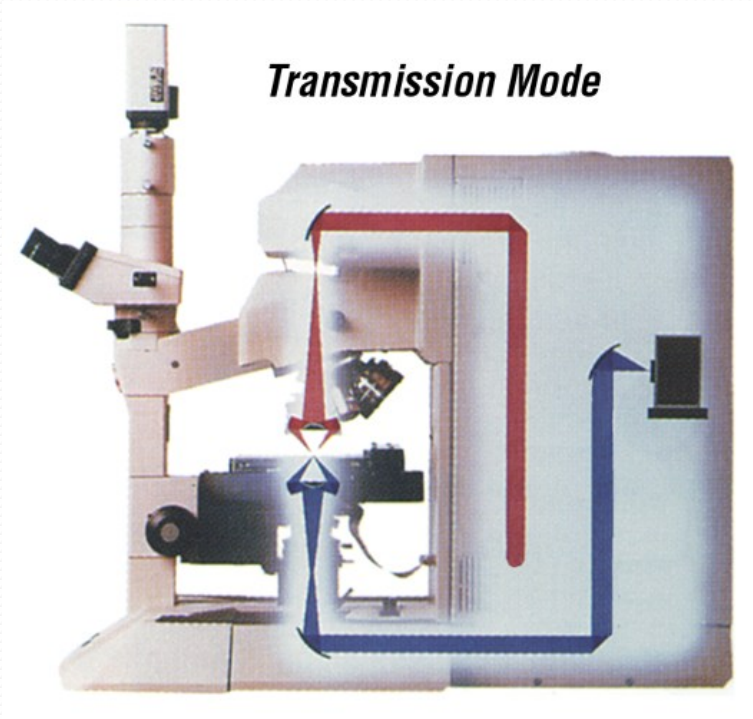

Reflection

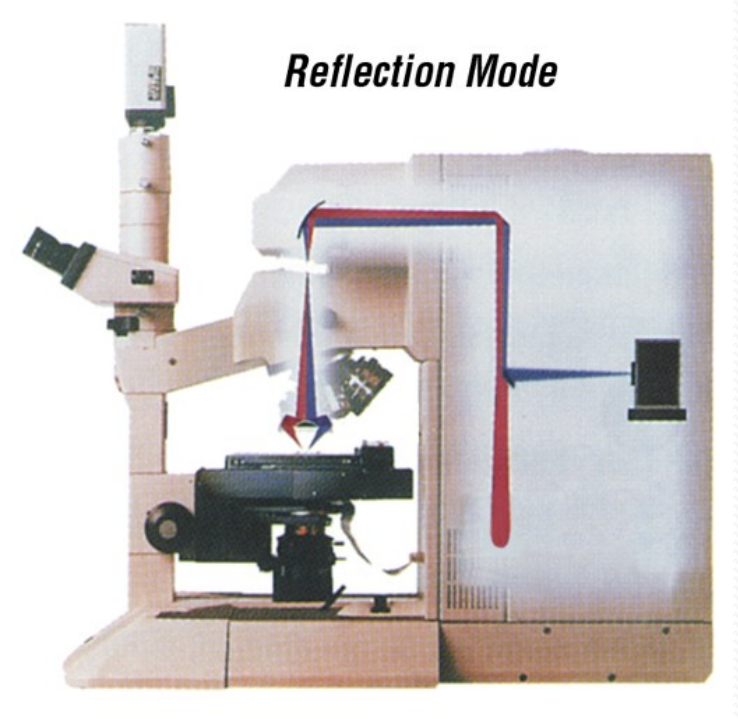

IR Microspectroscopy Sampling Modes

Transmission

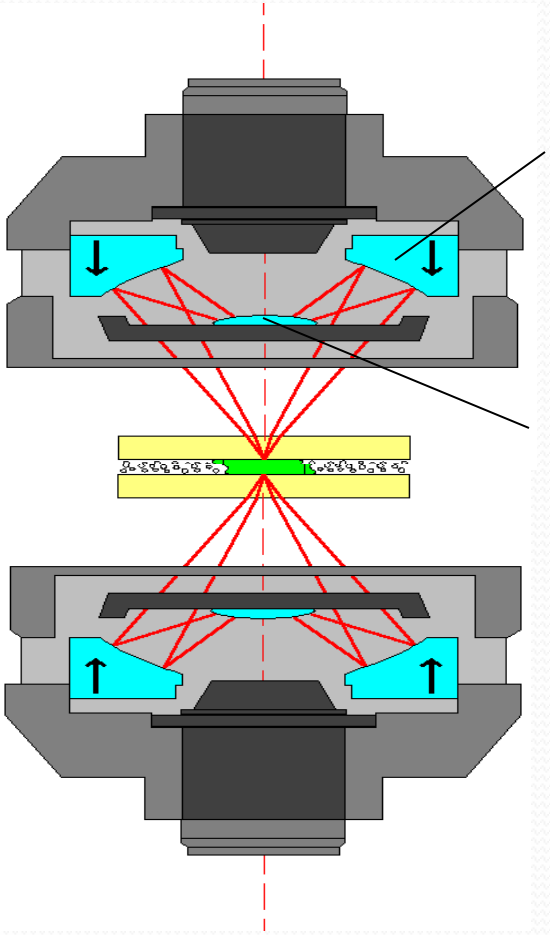

Reflection

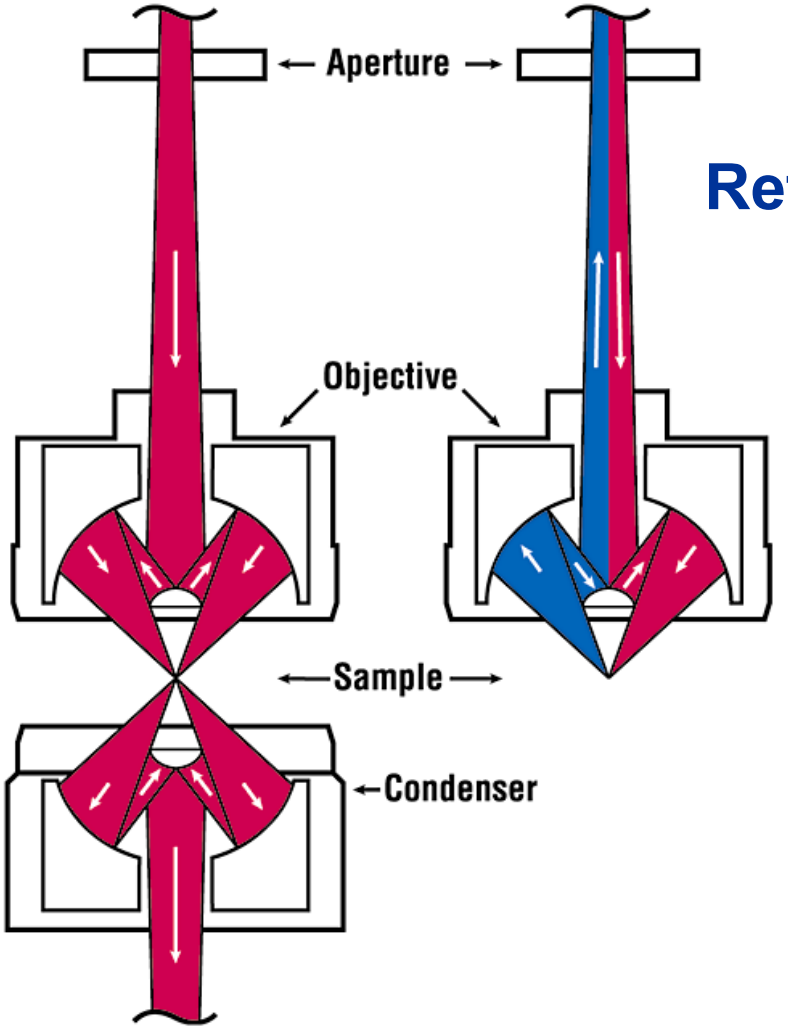

IR Microspectroscopy Sampling Modes

Transmission

- transparent samples, thin layers

Reflection

- ATR
- reflection - absorption, specular reflection, grazing angle

IR Microspectroscopy Sampling Modes

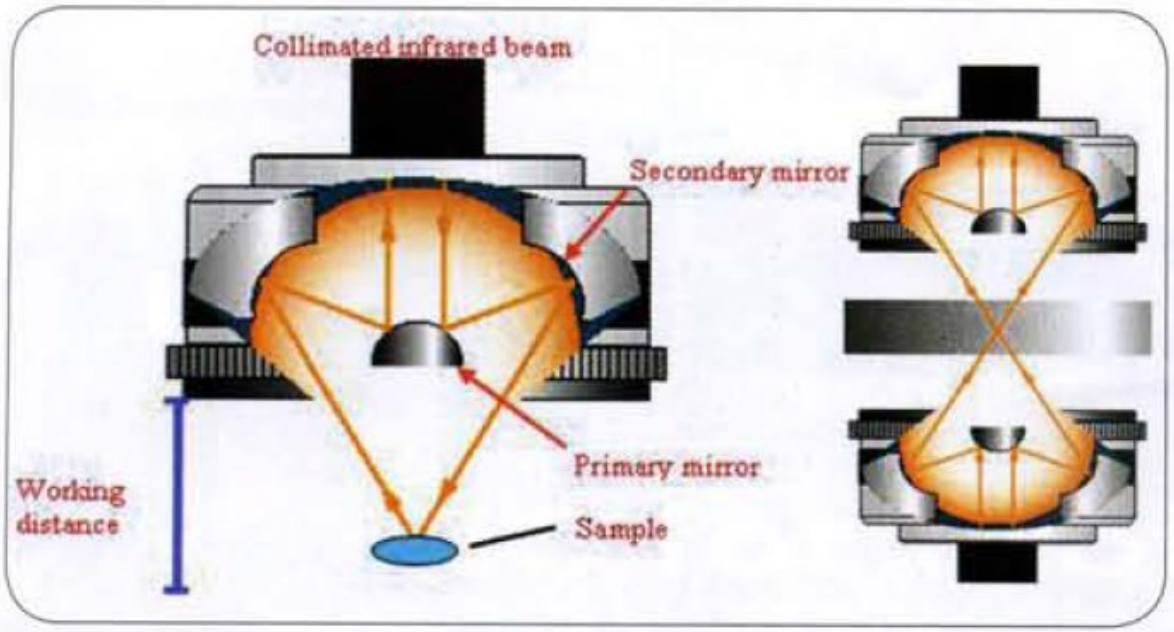

Transmission

- transparent samples, thin layers
  - 5 - 15 µm thickness
  - large and uniform surface

- mounting in compression cell between windows makes ideal transmission sample

IR Microspectroscopy Sampling Modes

Reflection - ATR

- simplifies sample preparation
- simplifies sample thickness problem
  (0.4 - 2.0 µm penetration depth)

- position sample on stage
- adjust for contact alert – contact sensor

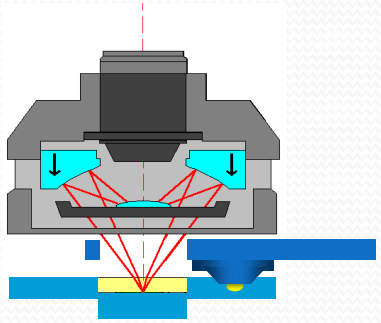

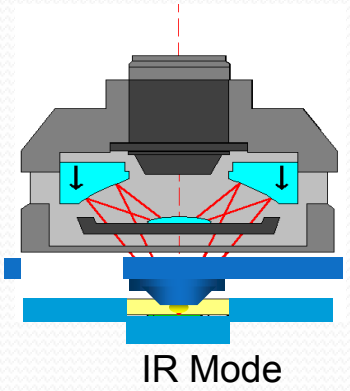

IR Microspectroscopy Sampling Modes

Technical specifications

	Ge Hemispherical	Si Hemispherical	Ge Conical Tip
Material	Germanium	Silicon	Germanium
Refraction index	4	3.4	4
Depth of penetration @ 2000 cm^{-1}	0.4 micron	0.6 micron	0.8 micron
Medium angle of incidence	55 degrees	55 degrees	25 degrees
Contact area diameter	120 micron	120 micron	100 micron
Typical sample area	25 micron	25 micron	25 micron
Minimum sample area*	12 micron	12 micron	< 10 micron
Crystal probe length	2.5 mm	2.5 mm	6 mm
Survey ATR	Yes	Yes	Yes
Spectral range cut-off	650 cm^{-1}	650 cm^{-1}	650 cm^{-1}

** Note: Minimum sample area is typically achieved with a Continuum aperture size of 30 x 30 micron divided by the crystal refractive index.*

IR Microspectroscopy Sampling Modes

Reflection - ATR

- objective crystals - ZnSe, Ge, Si, Diamond

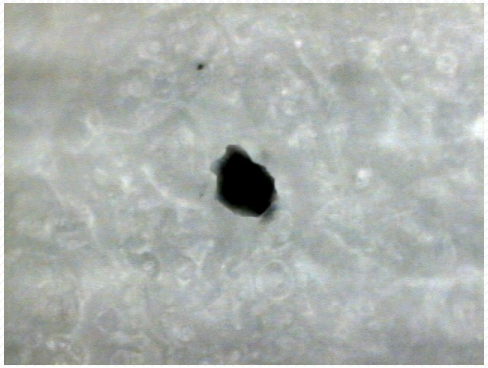

40 µm defect

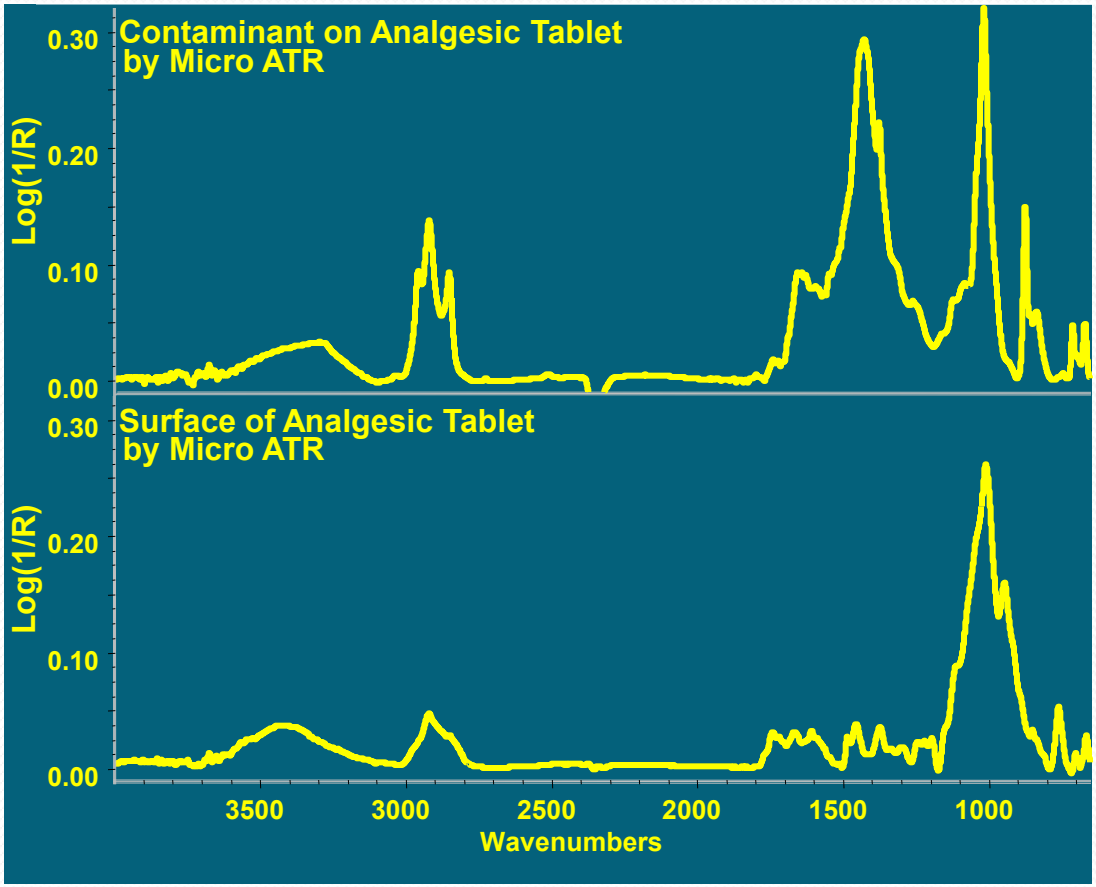

IR Microspectroscopy Sampling Modes

Reflection – grazing angle

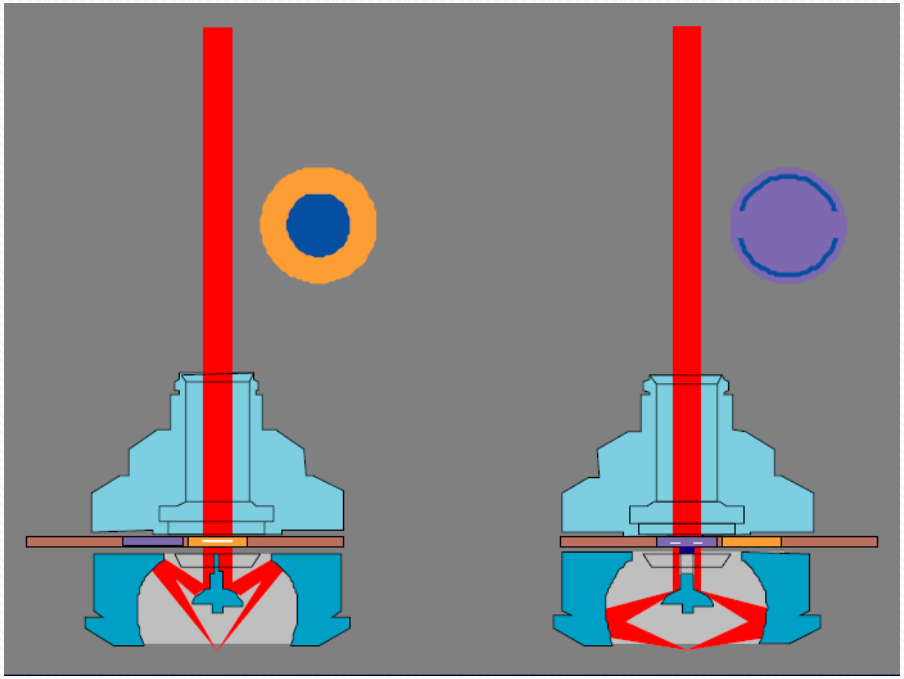

Polymer Laminate Spectra

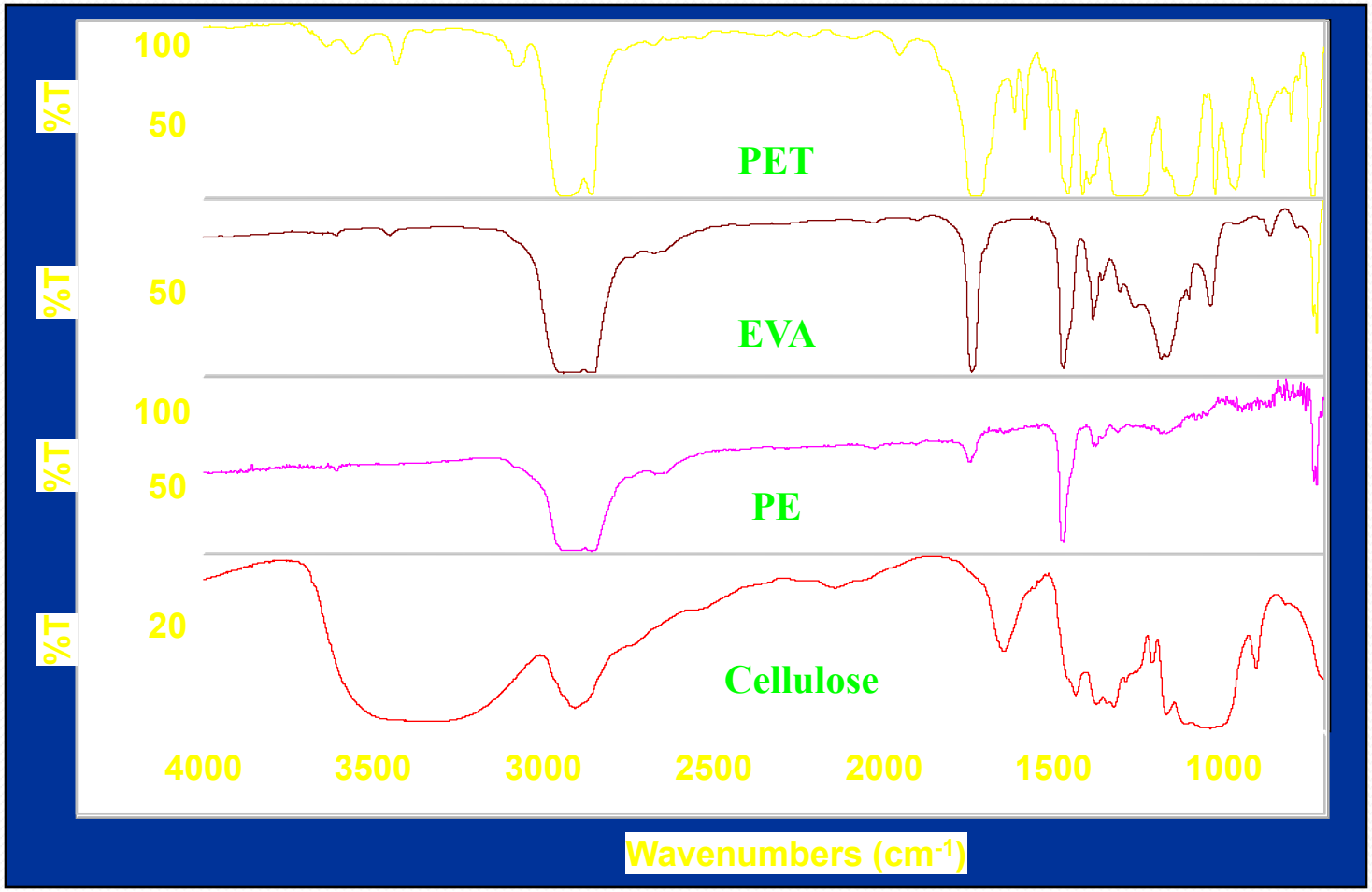

FTIR mikrospektroskopie – příklad

FTIR imaging microscope for chemical composition and spatial info at the cellular scale. Gives info like **lignin**, **starch**, **protein** and **oil** distribution.

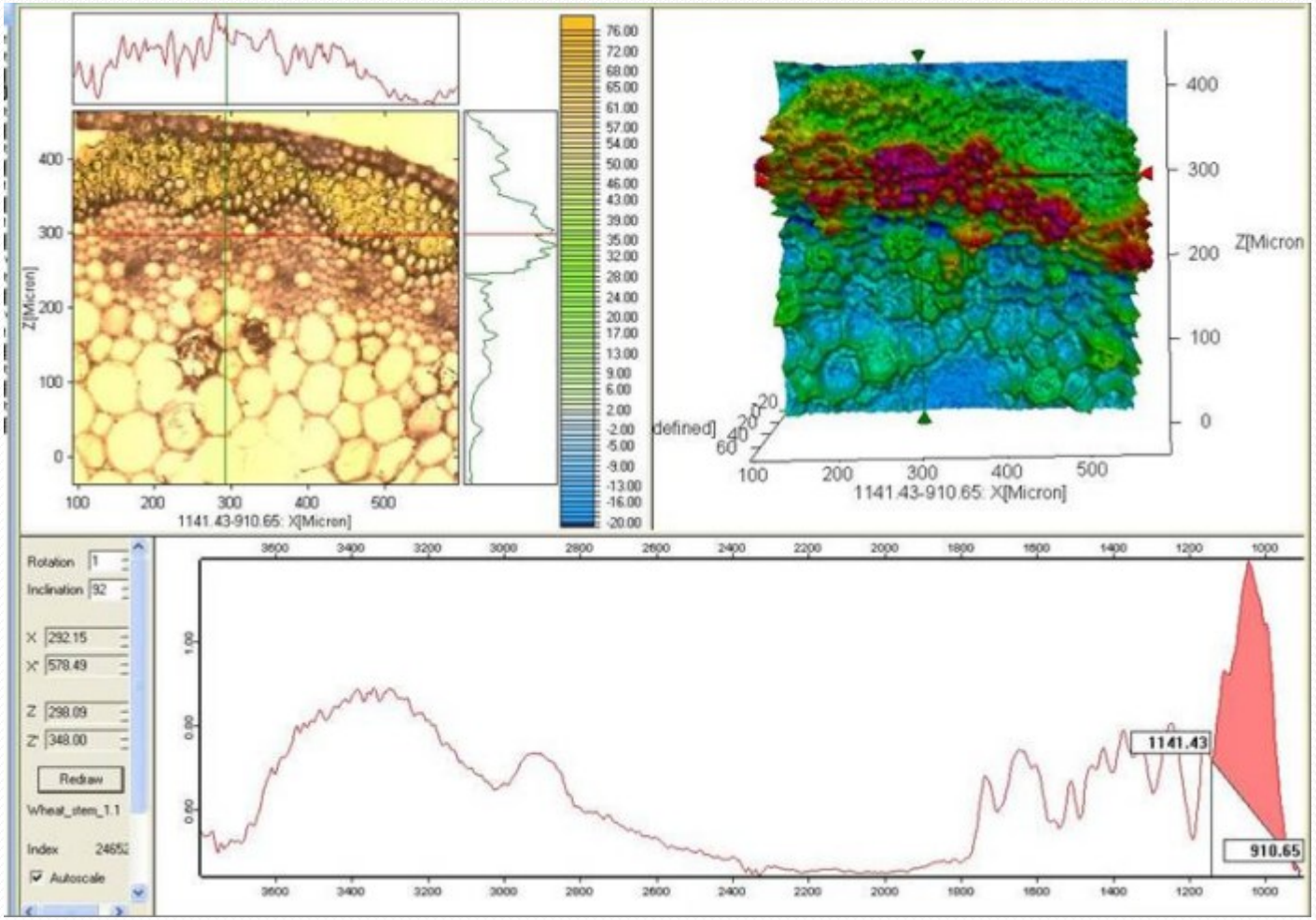

Hindawi Publishing Corporation
International Journal of Spectroscopy
Volume 2009, Article ID 893528, 5 pages
doi:10.1155/2009/893528

Research Article

The Use of FTIR and Micro-FTIR Spectroscopy: An Example of Application to Cultural Heritage

Mauro Francesco La Russa,[1] Silvestro Antonio Ruffolo,[1] Germana Barone,[2] Gino Mirocle Crisci,[1] Paolo Mazzoleni,[2] and Antonino Pezzino[2]

Samples	Sampling points and typology of degradation products
Sar1	Central *clipeo*, right side, black crust
Sar 2	Sixth *strigile*, at right-high side of *clipeo* black crust
Sar 4	Higher left side, orange patinas
Sar 5a	Inside left area, black crust
Sar 5b	Inside left area, orange patinas

(a) (b)

FIGURE 1: (a) The Roman sarcophagus; (b) particular of the facade of St. Giuseppe Church.

gradation products

SG1	Calcarenite with black crust localized on the base of column right
SG2	Calcarenite with black crust localized on the base of column left
SG3	Calcarenite with black crust localized on the portal
SG4	Brown-orange patinas present on the facade
SG5	Brown-orange patinas present on the facade
SG6	Brown-orange patinas present on the facade

Fourier transform-infrared spectroscopy (FTIR) was performed for a mineralogical characterization of the powdered samples by means of comparison to a data base [10]. The equipment used was a Nicolet 380 with a Smart Orbit accessory used in the following arrangement: a K-Br beam-splitter, an HP-DTGS-KBr detector, and an Ever-Glow lamp used as source. In this configuration, the resolution was 4 cm^{-1}. The great advantage of this spectroscopic technique is the high sensibility which allows the detection of many components, even at very low amounts.

The qualitative distribution maps of mineralogical phases, performed on thin sections, have been obtained by using a micro-Fourier transform-infrared spectrometer (μ-FTIR) Spotlight 200 (Perkin Elmer) microscope, equipped with an MCT detector cooled by liquid nitrogen, a germanium μATR crystal, and a computer-controlled mapping stage programmable in the x and y directions. The spectra were recorded at 4 cm^{-1} resolution, mode with a spot of $100 \times 100\,\mu m^2$.

Point-by-point spectral mapping of the thin section was carried out in a grid pattern with the computer-controlled microscope stage with a spot of $100\,\mu m \times 100\,\mu m$. Each spectrum was collected between 4000 and 700 cm^{-1} at a spectral resolution of 4 cm^{-1}. The map spectra were collected with 4 scans for each spectrum. Maps have a resolution of 625 dots and a spatial resolution of 100 μm. They are based on the compare correlation value (calculated by Spotlight 200 software) of the recorded spectra with references ones. A compare correlation map indicates the areas of a map, where the spectra are most similar to a reference spectrum.

Hindawi Publishing Corporation
International Journal of Spectroscopy
Volume 2009, Article ID 893528, 5 pages
doi:10.1155/2009/893528

Research Article

The Use of FTIR and Micro-FTIR Spectroscopy: An Exan Application to Cultural Heritage

Mauro Francesco La Russa,[1] Silvestro Antonio Ruffolo,[1] Germana Barone,[2] Gino Mirocle Crisci,[1] Paolo Mazzoleni,[2] and Antonino Pezzino[2]

FIGURE 1: (a) The Roman sarcophagus; (b) particular of the facade of St. Giuseppe Church.

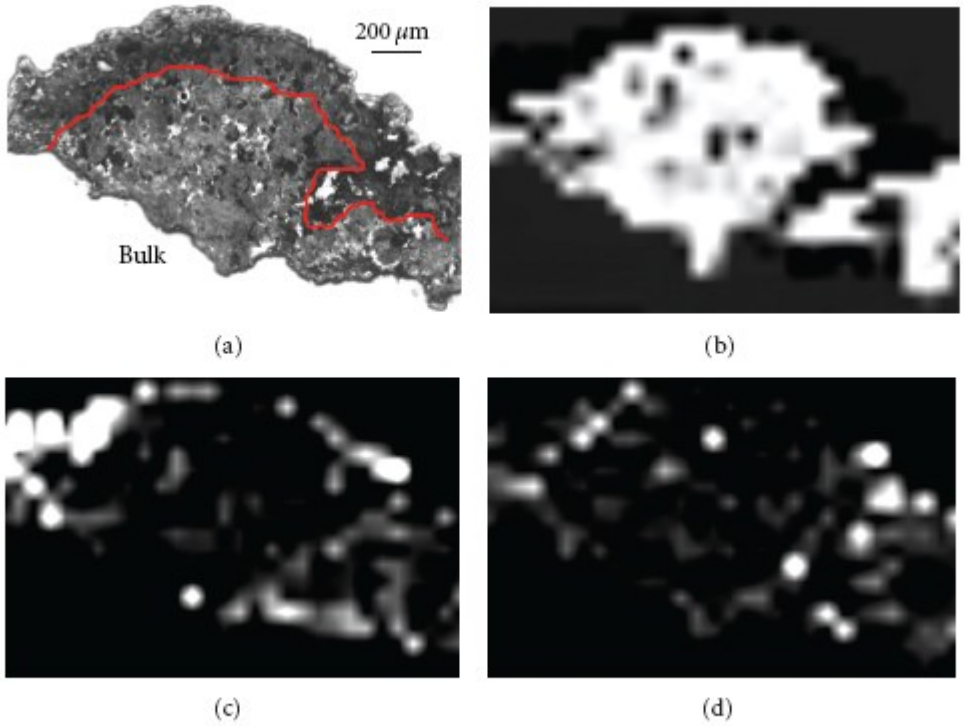

FIGURE 3: (a) Ultrathin section analyzed, (b) distribution maps of calcite, (c) gypsum, and (d) whewellite obtained by μ-FTIR-ATR spectroscopy. The bright areas indicate regions of high concentration, while dark areas indicate a low concentration.

Hindawi Publishing Corporation
International Journal of Spectroscopy
Volume 2009, Article ID 893528, 5 pages
doi:10.1155/2009/893528

Research Article

The Use of FTIR and Micro-FTIR Spectroscopy: An Example of Application to Cultural Heritage

Mauro Francesco La Russa,[1] Silvestro Antonio Ruffolo,[1] Germana Barone,[2] Gino Mirocle Crisci,[1] Paolo Mazzoleni,[2] and Antonino Pezzino[2]

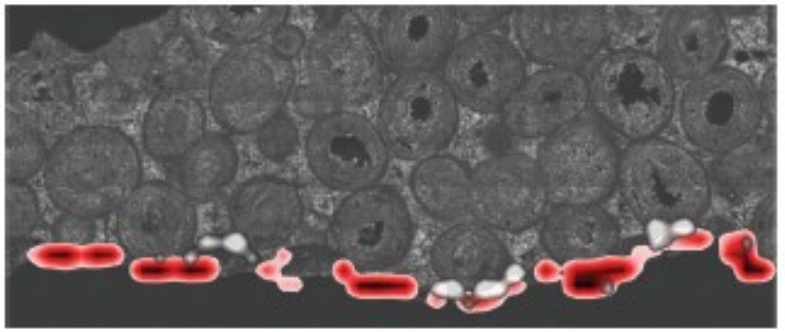

FIGURE 5: Thin section analyzed. Distribution map gypsum (light to dark red) and calcium oxalate (grey to white) obtained by μ-FTIR-ATR.

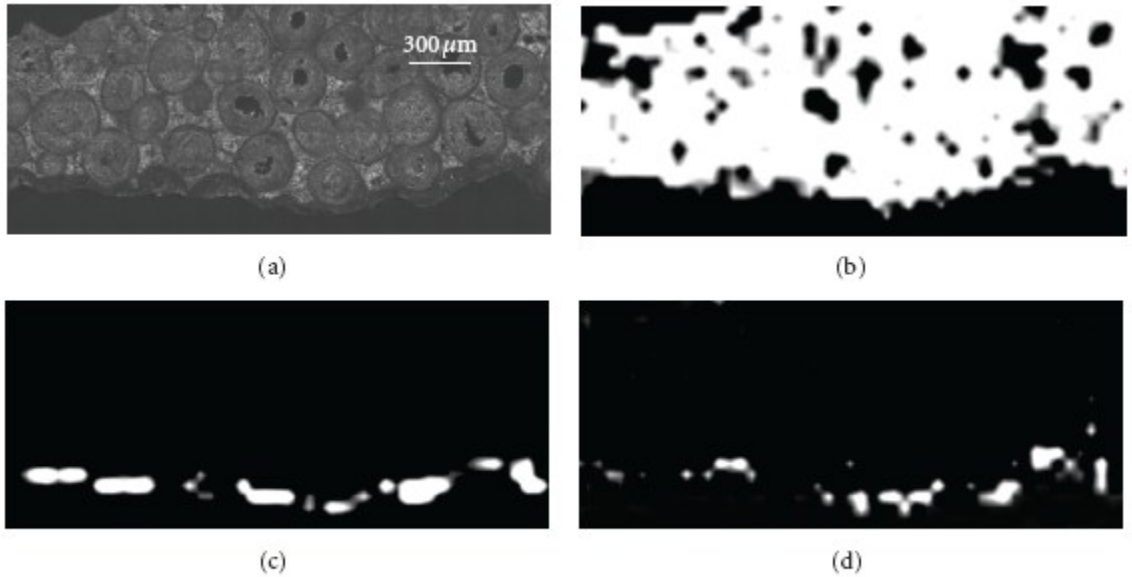

FIGURE 4: (a) Thin section analyzed (b) distribution maps of calcite, (c) gypsum, and (d) calcium oxalate obtained by μ-FTIR-ATR. The bright areas indicate regions of high concentration, while dark areas indicate a low concentration.

Available online at www.sciencedirect.com
ScienceDirect
Journal of Cultural Heritage 8 (2007) 339–349
Journal of Cultural Heritage
http://france.elsevier.com/direct/CULHER/

Original article

Non-destructive methods for chemical, optical, colorimetric and typographic characterisation of a reprint

Klementina Možina [a,*], Marjeta Černič [b], Andrej Demšar [c]

For comparison of the chemical composition of both papers, the FTIR spectroscopy technique was used. FTIR (Fourier Transform Infrared Spectroscopy) spectra of both papers using the ATR (Attenuated Total Reflection) technique [18,19] were recorded on a Perkin Elmer Fourier transform infrared spectrometer equipped with a DTGS detector. The Specac Golden Gate single reflection Attenuated Total Reflectance System (ATR) was mounted into the sample compartment. The ATR system was fitted with a diamond crystal and operated with single reflection optics at an interaction angle of 45°. The samples of paper were pressed against the crystal and thirty-two scans were collected for each measurement over the spectral range of 4000–500 cm^{-1} with a resolution of 4 cm^{-1} in order to obtain the spectra of both papers.

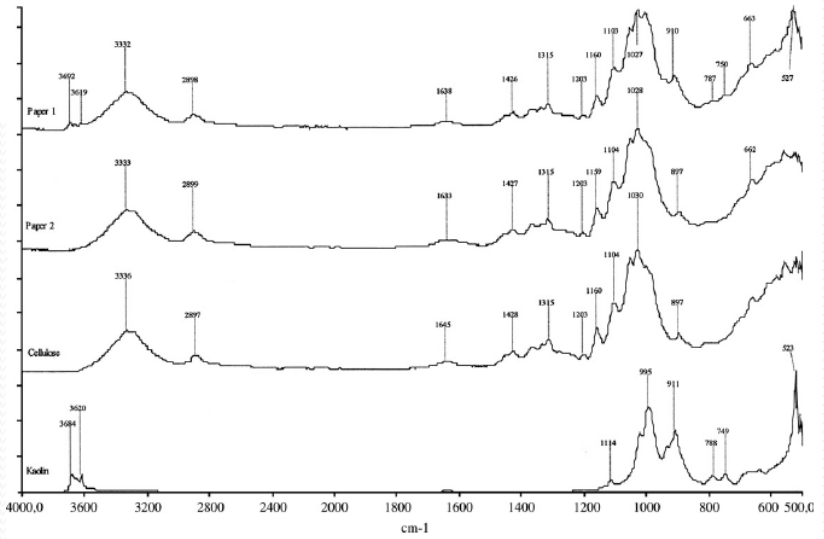

Fig. 2. FTIR–ATR spectra of paper 1 (Book 1), paper 2 (Book 2), cellulose, and kaolin.

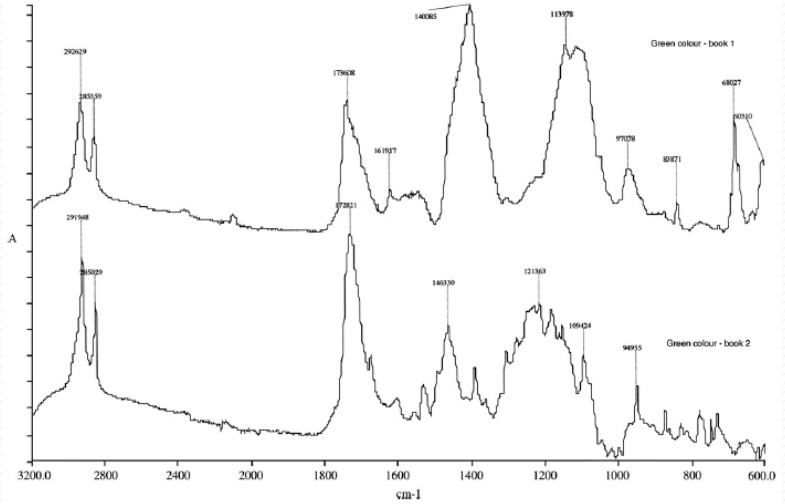

Fig. 6. FTIR–ATR spectra of green colour prints (without background—paper) in Book 1 and Book 2.

ANALYTICA CHIMICA ACTA 630 (2008) 141–149

available at www.sciencedirect.com

ScienceDirect

journal homepage: www.elsevier.com/locate/aca

Benefits of applying combined diffuse reflectance FTIR spectroscopy and principal component analysis for the study of blue tempera historical painting

Natalia Navas[a,*], *Julia Romero-Pastor*[b], *Eloisa Manzano*[a], *Carolina Cardell*[b]

[a] *Dept. of Analytical Chemistry, University of Granada, Fuentenueva s/n, 18071 Granada, Spain*
[b] *Dept. of Mineralogy and Petrology, University of Granada, Fuentenueva s/n, 18071 Granada, Spain*

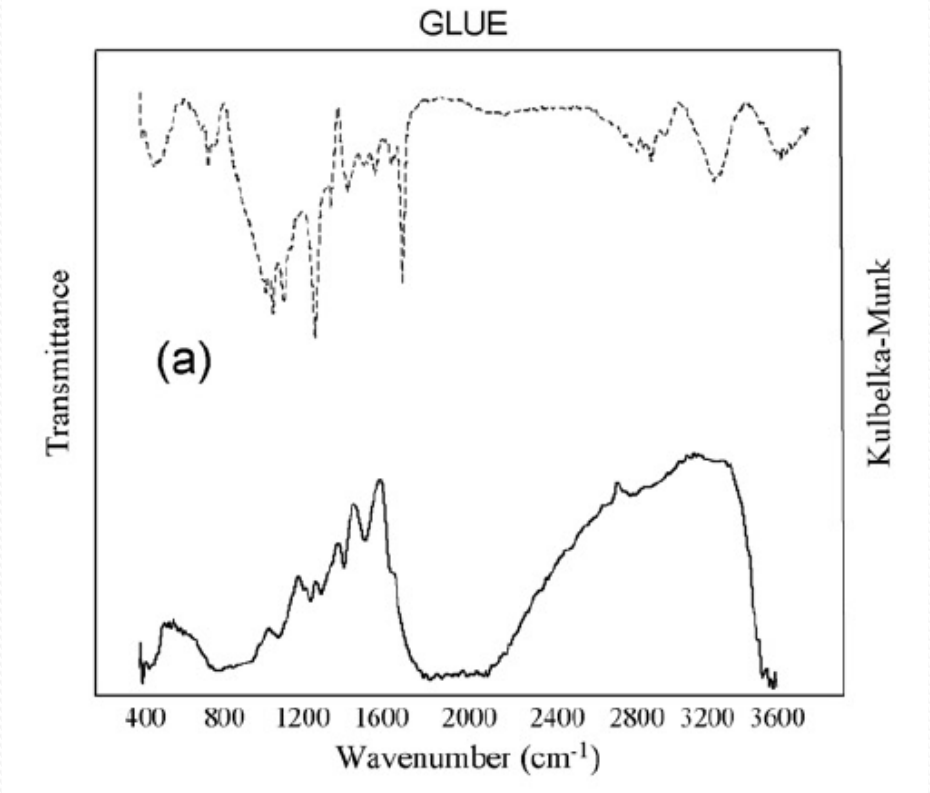

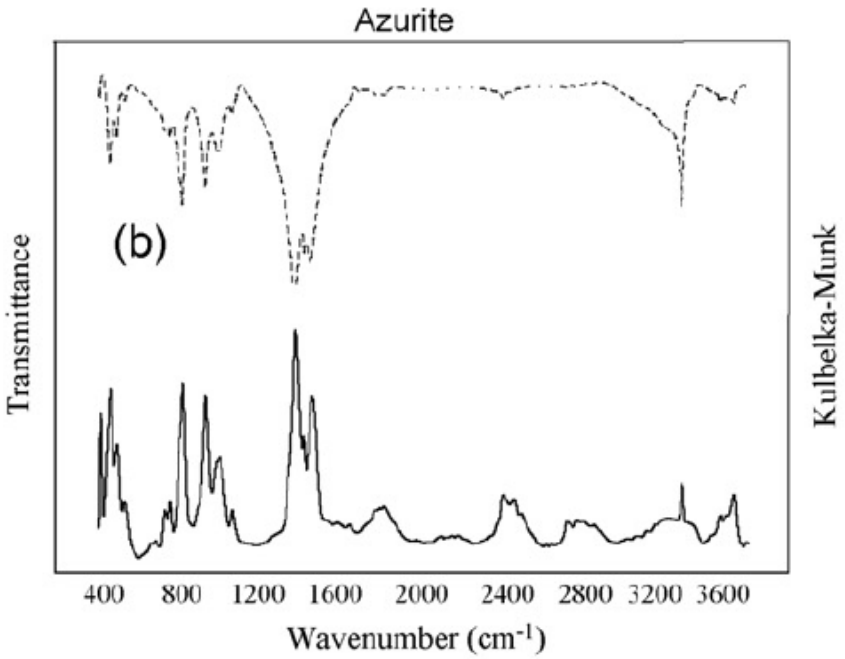

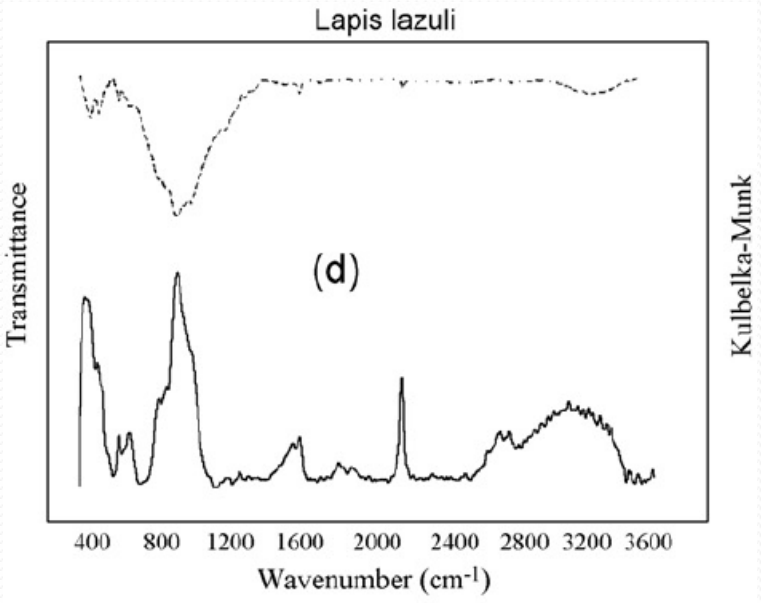

ANALYTICA CHIMICA ACTA 630 (2008) 141–149

available at www.sciencedirect.com

ScienceDirect

journal homepage: www.elsevier.com/locate/aca

Benefits of applying combined diffuse reflectance FTIR spectroscopy and principal component analysis for the study of blue tempera historical painting

Natalia Navas[a,*], *Julia Romero-Pastor*[b], *Eloisa Manzano*[a], *Carolina Cardell*[b]

[a] *Dept. of Analytical Chemistry, Univ*

[b] *Dept. of Mineralogy and Petrology,*

Table 2 – Main IR absorption bands of the blue pigments and their temperas for identifications purposes.

Replica sample	Description	Vibrational wavenumber (cm^{-1})	
		T-FTIR	DRIFT
Pure rabbit glue	Collagen	700 (δ (NH) wagging band) 1290 (amide band II) 1730 (amide band I) 3310 (N–H stretching mode)	680, 3000 [31]
Pure azurite	$Cu_3(CO_3)_2(OH)_2$	840 (carbonate stretching [28]) 1430 (carbonate stretching [28])	840 (as in T-FTIR) 1430 (as in T-FTIR)
Azurite/rabbit glue	$Cu_3(CO_3)_2(OH)_2$/collagen	840 (carbonate stretching [28]) 1430 (carbonate stretching [28])	840 (as in T-FTIR) 1430 (as in T-FTIR) 1890, 2510, 2890
Pure lapis lazuli	$Na_{8-10}Al_6Si_6O_{24}S_{2-4}$	460 (O–Si–O deformation mode [29,30]) 990 (O–Si–O anti-symmetric stretching mode [29,30])	460 (as in T-FTIR) 990 (as in T-FTIR)
Lapis lazuli/rabbit glue	$Na_{8-10}Al_6Si_6O_{24}S_{2-4}$/collagen	460 (O–Si–O deformation mode [29,30]) 990 (O–Si–O anti-symmetric stretching mode [29,30]) 1290 (amide band II) 1730 (amide band I)	460 (as in T-FTIR) 990 (as in T-FTIR)
Pure smalt	Potassium silicate glass with some cobalt oxide	480 (O–Si–O deformation mode [29,30]) 1030 (O–Si–O anti-symmetric stretching mode [29,30])	480 (as in T-FTIR) 1030 (as in T-FTIR)
Smalt/rabbit glue	Potassium silicate glass with some cobalt oxide/collagen	480 (O–Si–O deformation mode [29,30]) 1030 (O–Si–O anti-symmetric stretching mode [29,30]) 1290 (amide band II) 1730 (amide band I)	480 (as in T-FTIR) 1030 (as in T-FTIR)

ANALYTICA CHIMICA ACTA 630 (2008) 141–149

available at www.sciencedirect.com

ScienceDirect

journal homepage: www.elsevier.com/locate/aca

Benefits of applying combined diffuse reflectance FTIR spectroscopy and principal component analysis for the study of blue tempera historical painting

Natalia Navas[a,*], *Julia Romero-Pastor*[b], *Eloisa Manzano*[a], *Carolina Cardell*[b]

[a] Dept. of Analytical Chemistry, University of Granada, Fuentenueva s/n, 18071 Granada, Spain
[b] Dept. of Mineralogy and Petrology, University of Granada, Fuentenueva s/n, 18071 Granada, Spain

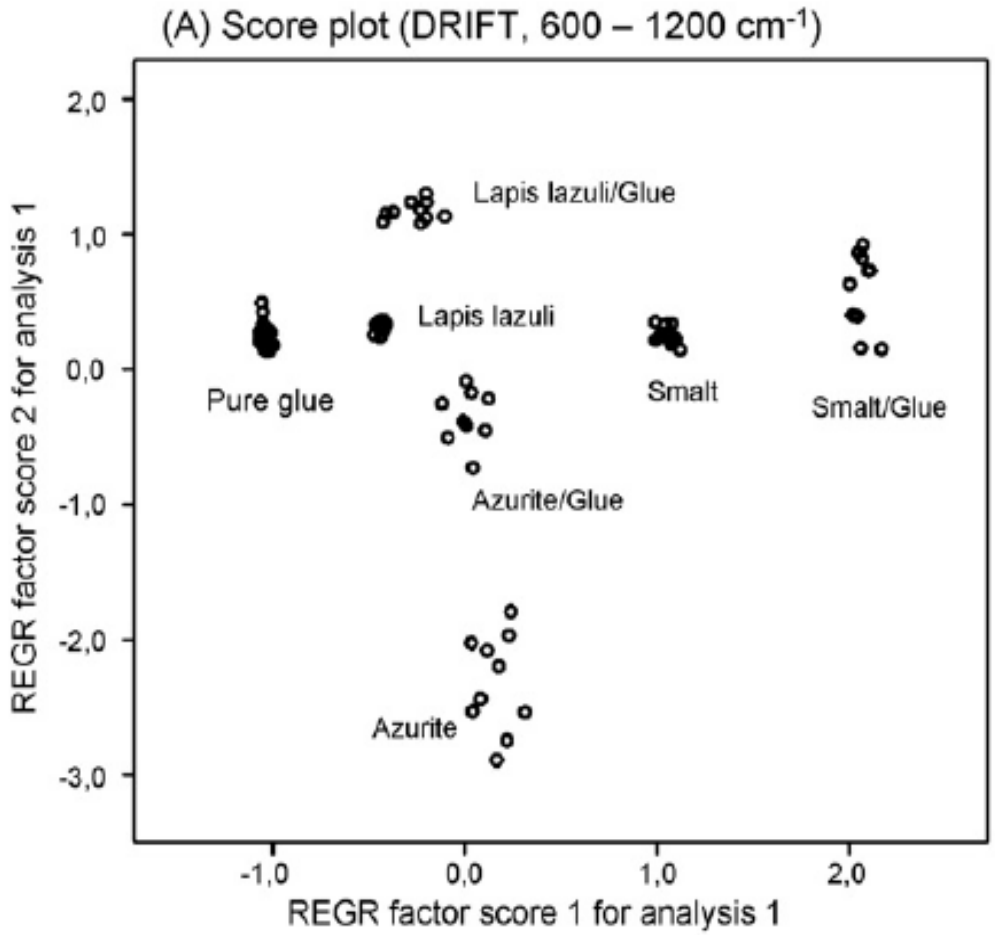

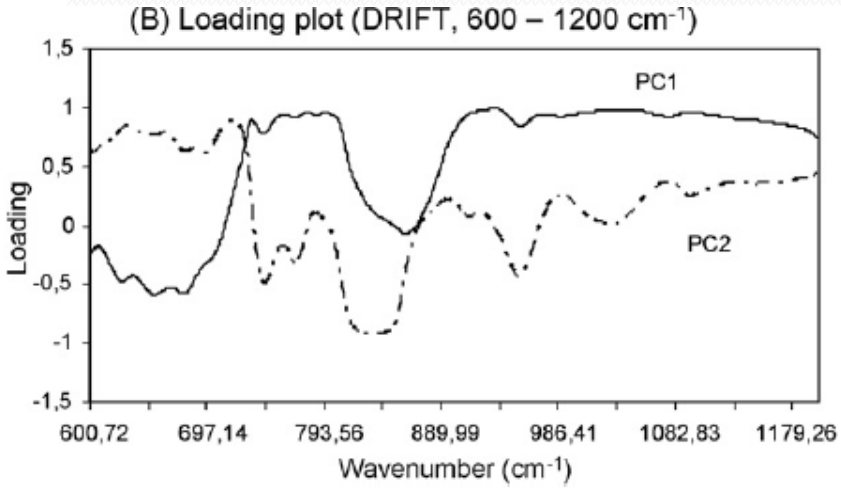

Available online at www.sciencedirect.com
ScienceDirect
C. R. Physique ••• (••••) •••–•••
COMPTES RENDUS PHYSIQUE
ELSEVIER

FTIR mikrospektroskopie – synchrotronové záření

Physics and heritage / Physique et patrimoine

Recent applications and current trends in Cultural Heritage Science using synchrotron-based Fourier transform infrared micro-spectroscopy

Marine Cotte [a,b,*], Paul Dumas [c], Yoko Taniguchi [d], Emilie Checroun [e], Philippe Walter [a], Jean Susini [b]

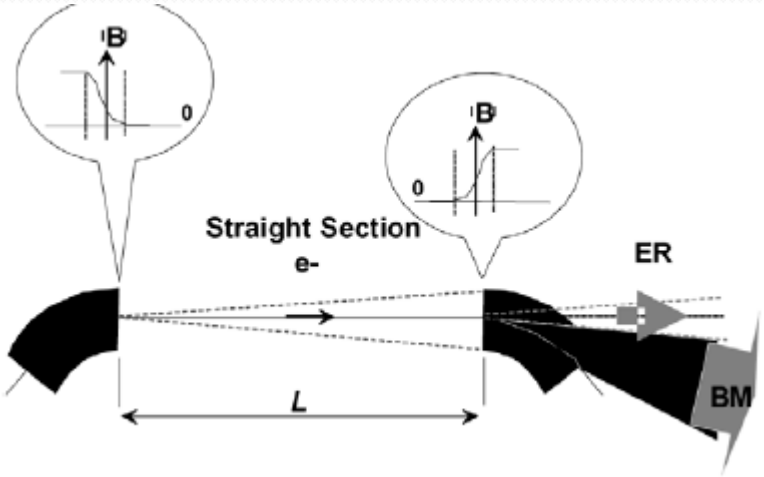

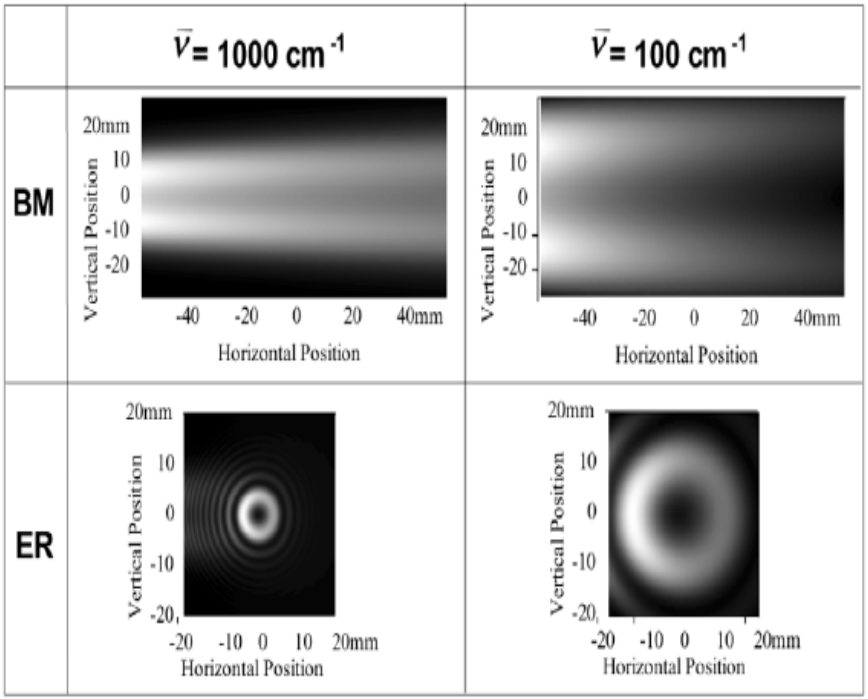

Fig. 2. Intensity distribution of edge radiation, for two wavelengths: $\lambda = 10$ μm (left column) and $\lambda = 100$ μm (right column). The distribution has been calculated for a bending magnet (BM) emission, and an edge radiation (ER) emission. This calculation has been carried out for the case of a storage ring of 3 GeV, and a vertical aperture of 20 mrad.

ELSEVIER

Available online at www.sciencedirect.com

ScienceDirect

C. R. Physique ••• (••••) •••–•••

COMPTES RENDUS PHYSIQUE

FTIR mikrospektroskopie – synchrotronové záření

Physics and heritage / Physique et patrimoine

Recent applications and current trends in Cultural Heritage Science using synchrotron-based Fourier transform infrared micro-spectroscopy

Marine Cotte [a,b,*], Paul Dumas [c], Yoko Taniguchi [d], Emilie Checroun [e], Philippe Walter [a], Jean Susini [b]

Flux and brightness for the two types of IR emission are almost equivalent, but the opening angle of the ER is narrower than that of the SR from constant field of a BM. The intensity profiles of the two types of emission are also different, and depend upon wavelength. In Fig. 2, the distribution profiles at two wavelengths (10 μm and 100 μm) have been calculated for a medium energy storage ring (3.0 GeV) for a prototypical opening angle of the dipole chamber of 20 × 40 mrad (vertical by horizontal) for the collection of BM infrared emission, and 20 × 20 mrad for the collection of the ER infrared emission. These profiles illustrate that, for BM emission, the angle of emission is larger than that of the ER. However, flux and brightness are equivalent for the two types of emission sources, and either one can be used for synchrotron infrared experiments.

This has some advantages for engineering purposes, since the dipole chamber exit port in a synchrotron storage ring has to be enlarged for BM radiation. Thus today, both sources are used for extraction, depending upon availability of a straight section and/or BM. The most recent synchrotron facilities are collecting both sources, and split them after the propagation to the instrument in order to have two spectroscopic branches with the same extraction port (Australian Synchrotron, SOLEIL, Diamond).

A marked difference between the two sources is their polarization properties. BM emission is strictly horizontally polarized in the plane of the electron trajectory, while ER has a radial polarization.

ELSEVIER

Available online at www.sciencedirect.com

ScienceDirect

C. R. Physique ••• (••••) •••–•••

COMPTES RENDUS PHYSIQUE

Physics and heritage / Physique et patrimoine

Recent applications and current trends in Cultural Heritage Science using synchrotron-based Fourier transform infrared micro-spectroscopy

Marine Cotte [a,b,*], Paul Dumas [c], Yoko Taniguchi [d], Emilie Checroun [e], Philippe Walter [a], Jean Susini [b]

FTIR mikrospektroskopie – synchrotronové záření

The IR light is then focused through an IR-transparent window (usually diamond, but in a few cases IR-transparent windows such as KBr, ZnSe and KRS5 have been used), which separates the ultra-high vacuum (UHV) conditions of the storage ring (10^{-9}–10^{-10} mbar) and the low vacuum of the SR-FTIR beamline (10^{-3}–10^{-4} mbar). This diamond window is usually a slight wedge shape to avoid interferences, and relatively small in diameter (10 to 40 mm clear aperture). Some sophisticated wheels containing windows of several materials (e.g. calcium fluoride, diamond, cesium iodide) have been recently implemented at the Swiss Light Source for the same purpose.

The low vacuum section of a SR-FTIR beamline is generally terminated with an IR-transparent window (KBr, CsI, polyethylene) either after a vacuum-based FTIR spectrometer or prior to a purged instrument. This window isolates the beamline vacuum from the ambient pressure of the spectrometer and/or microscope. To date, all commercial FTIR microscopes operate at ambient pressure and are typically purged with dry N_2 or dry air to remove any water vapor and carbon dioxide in the FTIR spectrum.

Available online at www.sciencedirect.com
ScienceDirect
C. R. Physique ••• (••••) •••–•••
COMPTES RENDUS PHYSIQUE
ELSEVIER

FTIR mikrospektroskopie – synchrotronové záření

Physics and heritage / Physique et patrimoine

Recent applications and current trends in Cultural Heritage Science using synchrotron-based Fourier transform infrared micro-spectroscopy

Marine

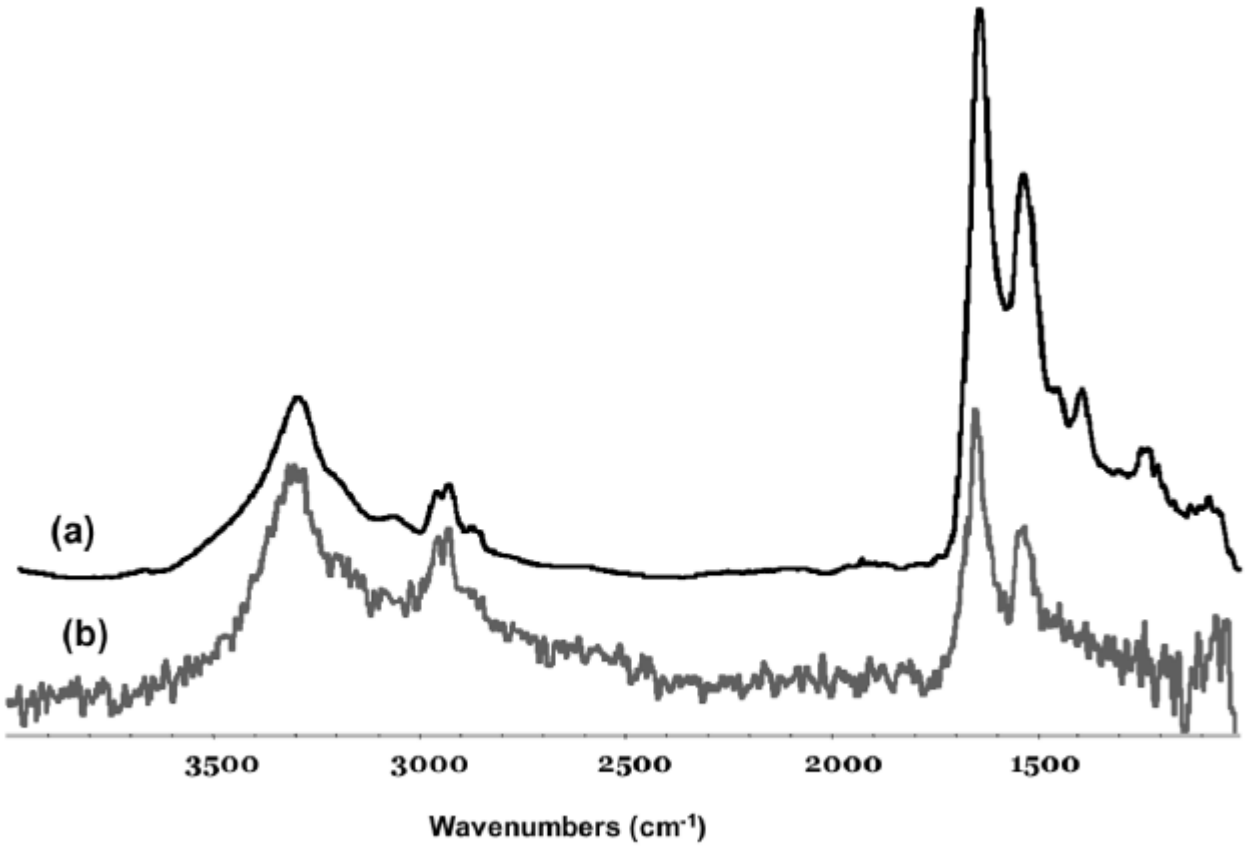

Fig. 4. FTIR spectra recorded with a dual aperture of $6 \times 6\ \mu m^2$, at $4\ cm^{-1}$ resolution, derived from a sum of 128 scans with (a) the synchrotron source and (b) with the internal (globar) source.

ELSEVIER

Available online at www.sciencedirect.com

ScienceDirect

C. R. Physique ••• (••••) •••–•••

COMPTES RENDUS PHYSIQUE

Physics and heritage / Physique et patrimoine

FTIR mikrospektroskopie – synchrotronové záření

Recent applications and current trends in Cultural Heritage Science using synchrotron-based Fourier transform infrared micro-spectroscopy

Marine Cotte [a,b,*], Paul Dumas [c], Yoko Taniguchi [d], Emilie Checroun [e], Philippe Walter [a], Jean Susini [b]

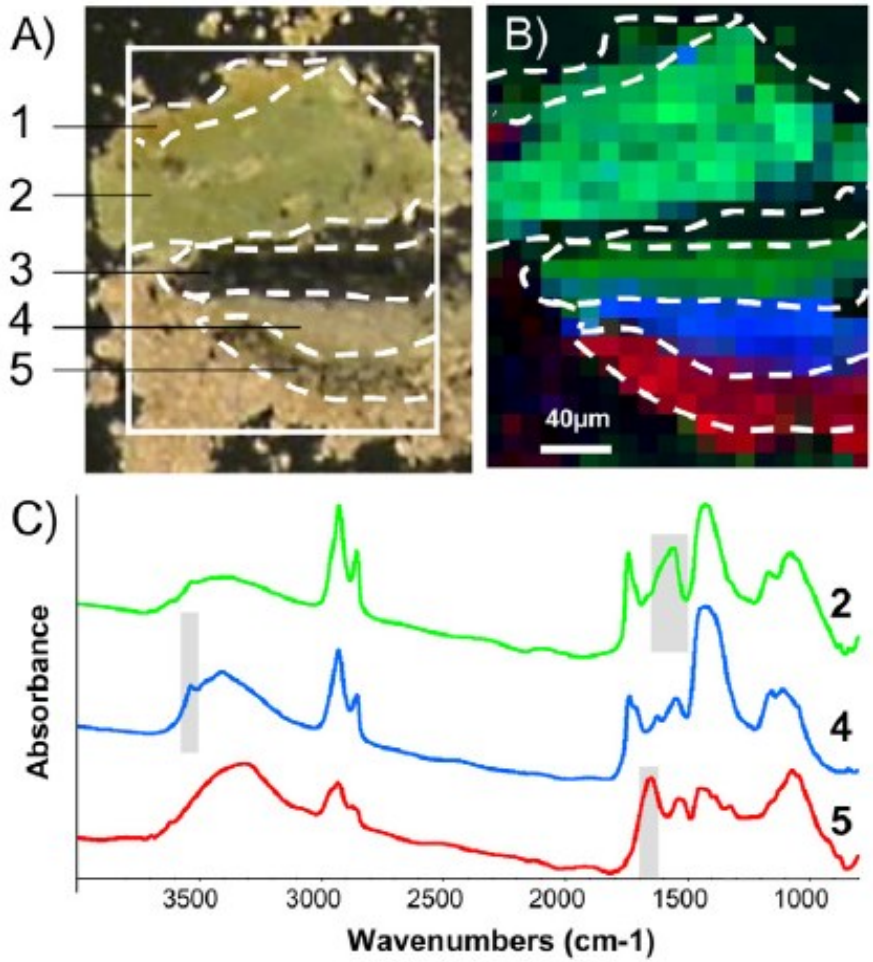

Fig. 5. A) Photomicrograph of pressed fragment of sample BMM035 from Cave N(a), Bamiyan, showing a multi-layered structure: 1 = yellowish transparent layer, 2 = green layer, 3 = black layer, 4 = white ground, 5 = transparent brownish layer, and earthen rendering. B) Chemical mappings obtained by SR-µFTIR, showing the distribution of three particular ingredients: in red, proteins; in green, carboxylates; in blue, hydrocerussite. Map size: 190 × 170 µm^2; step size: 10 × 10 µm^2. C) Average FTIR spectra obtained in the green layer (#2), the white ground layer (#4) and the transparent brownish layer (#5). The gray rectangles highlight the vibrational bands used to generate chemical mappings displayed in B).

FTIR mikrospektroskopie – srovnání s dalšími metodami

Available online at www.sciencedirect.com
ScienceDirect
C. R. Physique ••• (••••) •••–•••
COMPTES RENDUS PHYSIQUE
ELSEVIER

Physics and heritage / Physique et patrimoine

Recent applications and current trends in Cultural Heritage Science using synchrotron-based Fourier transform infrared micro-spectroscopy

Marine Cotte [a,b,*], Paul Dumas [c], Yoko Taniguchi [d], Emilie Checroun [e], Philippe Walter [a], Jean Susini [b]

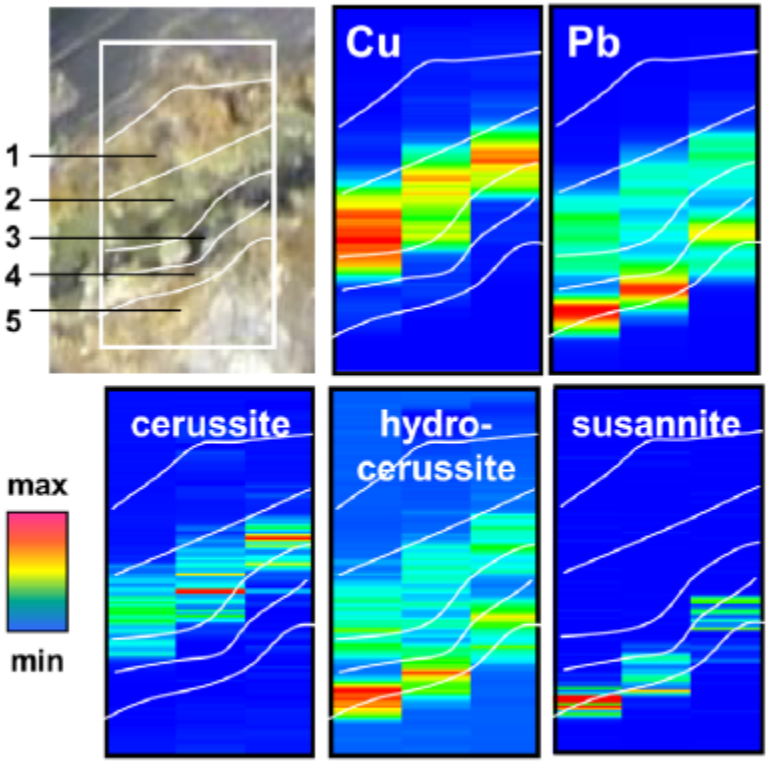

Fig. 6. Photomicrograph of sliced cross-section of sample BMM035 from Cave N(a), Bamiyan, showing a multi-layered structure: 1 = yellowish transparent layer, 2 = green layer, 3 = black layer, 4 = white ground, 5 = transparent brownish layer, and earthen rendering. Elemental and phase mappings obtained by μXRF and μXRD, respectively. Map size: 80 × 140 μm^2; beam and step size: 15 × 1 μm^2.

Available online at www.sciencedirect.com
ScienceDirect
C. R. Physique ••• (••••) •••–•••
COMPTES RENDUS PHYSIQUE
ELSEVIER
Physics and heritage / Physique et patrimoine

Recent applications and current trends in Cultural Heritage Science using synchrotron-based Fourier transform infrared micro-spectroscopy

Marine Cotte [a,b,*], Paul Dumas [c], Yoko Taniguchi [d], Emilie Checroun [e], Philippe Walter [a], Jean Susini [b]

FTIR mikrospektroskopie – srovnání s dalšími metodami

6. Conclusion

Even if most of experiments performed on synchrotron facility exploit the X-ray domain, the interest of IR micro-spectroscopy is clearly manifested in CH Science. Its main assets are the capacity to simultaneously probe inorganic and organic materials, even in an amorphous state; and to identify and to localize them with a rather good lateral resolution. In the field of CH, these advantages are particularly beneficial in the case of hybrid materials (paintings, varnishes, cosmetics but also ancient biological samples). No doubt that synchrotron-based FTIR will find many occasions to help solving ancient craftsmen's and artist's secrets.

Raman microscopy is also an excellent approach to vibrational spectroscopy, with an equivalent, or often better, spatial resolution than synchrotron infrared microscopy. Being more sensitive to the mineral compounds than IR, the dual use of such vibrational techniques offers a wide range of complementarities in Cultural Heritage Science. The data are complementary, but often Raman does not provide adequate spectral quality (i.e. signal to noise), data can be complicated by intrinsic fluorescence emission, and samples can suffer from laser beam damage. Thus, it is valuable to combine the two vibrational micro-spectroscopic approaches, and this should be made available for users at synchrotron facilities, such as at SOLEIL Infrared beamline.

Anal. Chem. **2005,** *77,* 3444−3451

Advantages of the Use of SR-FT-IR Microspectroscopy: Applications to Cultural Heritage

Nati Salvadó,*,† Salvador Butí,† Mark J. Tobin,‡ Emmanuel Pantos,‡ A. John N. W. Prag,§ and Trinitat Pradell⊥

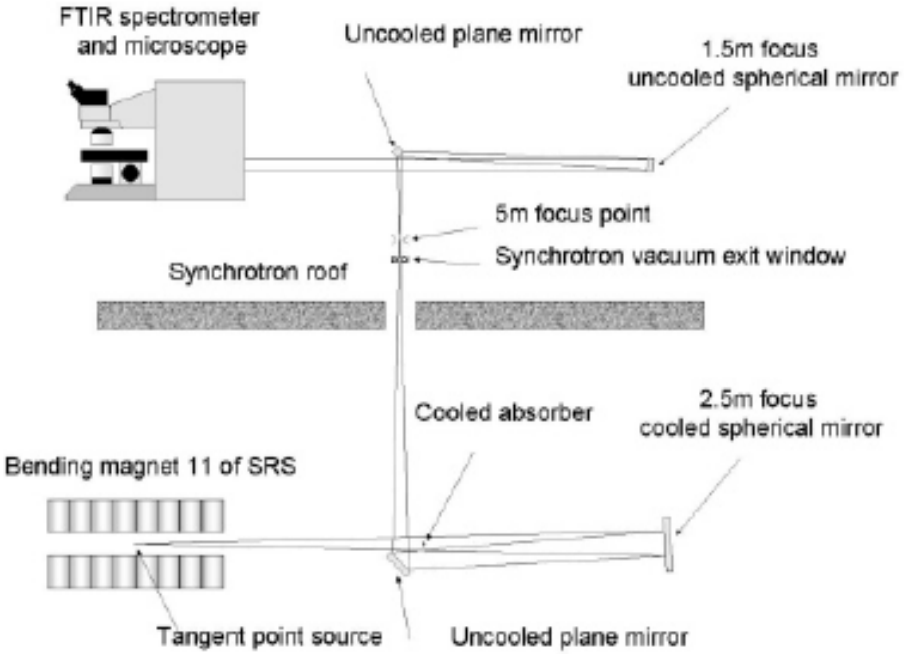

Figure 1. Schematic diagram of the SR-FT-IR beamline 11.1 at the Synchrotron Radiation Source, Daresbury Laboratory, Warrington, UK.

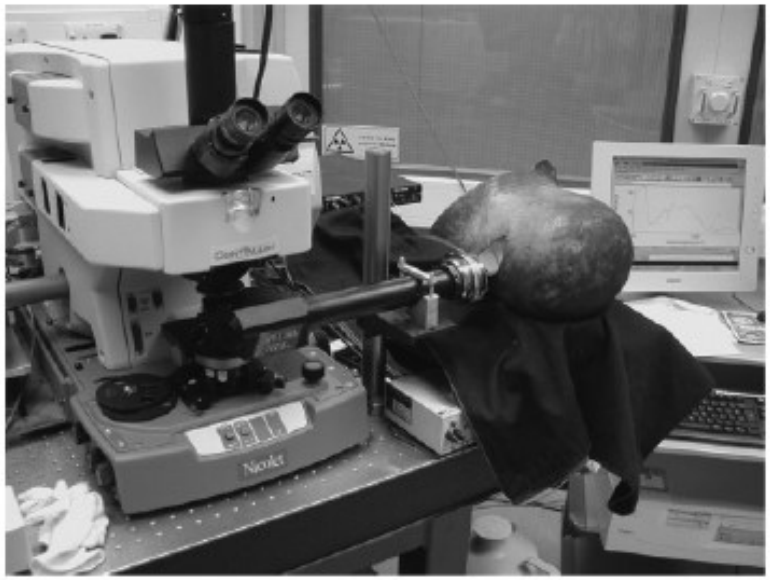

Figure 2. Photo of the instrument (spectrophotometer and microscope) and accessories used in order to collect spectra of large objects in reflection mode.

Anal. Chem. 2005, 77, 3444−3451

Advantages of the Use of SR-FT-IR Microspectroscopy: Applications to Cultural Heritage

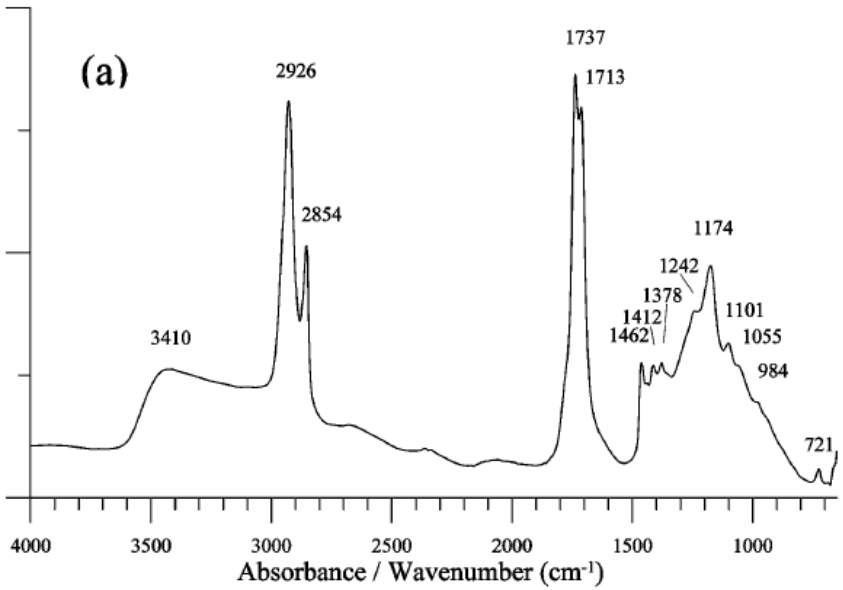

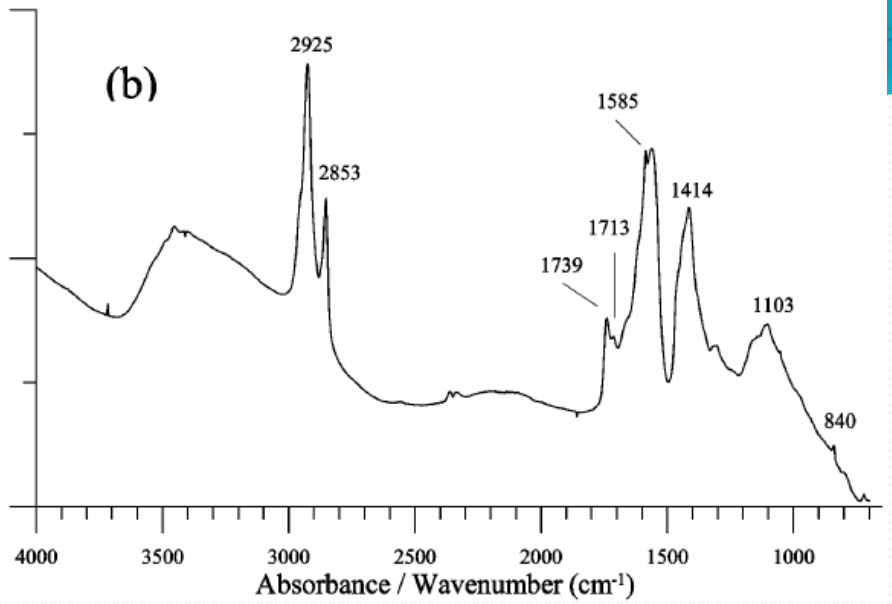

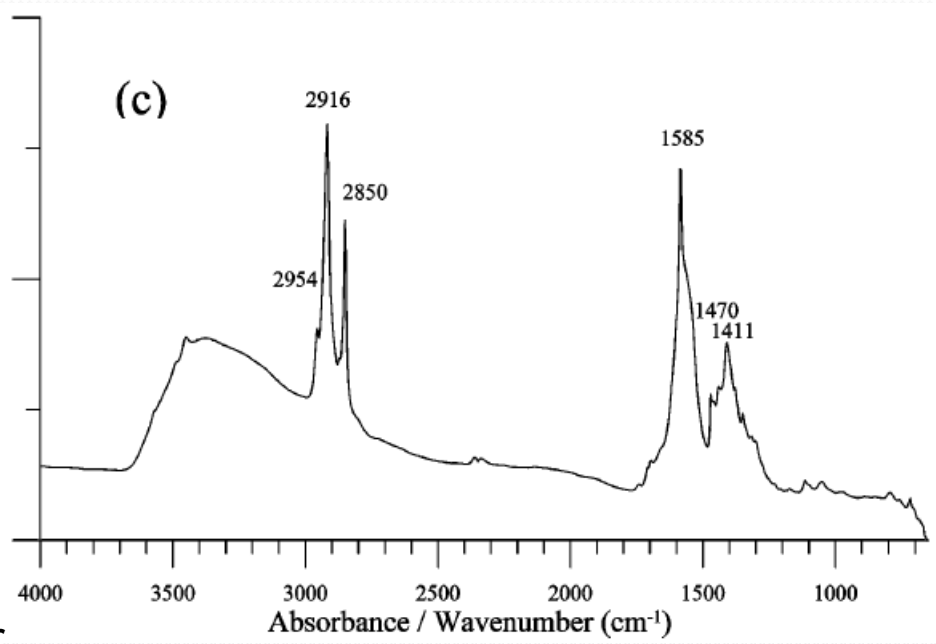

SR-FT-IR microspectroscopy spectra (128 scans, 4 cm^{-1} resolution, spot size 10 *μm 10 μm corresponding to (a) linseed drying* oil aged for 7 years; (b) green paint taken from the altarpiece “El Conestable” from Jaume Huguet (15th century AD) where a mixture of bands
related to an aged linseed drying oil and a metal carboxylate are identified; (c) copper carboxylate isolated from the green paint

Journal of Molecular Structure 924–926 (2009) 404–412

Comparison between micro-Raman and micro-FTIR spectroscopy techniques for the characterization of pigments from Southern Spain Cultural Heritage

M.L. Franquelo [a,*], A. Duran [a,b], L.K. Herrera [a], M.C. Jimenez de Haro [a], J.L. Perez-Rodriguez [a]

The FTIR absorbance measurement was performed in a range of wavenumbers between 700 and 3000 cm^{-1}, using a Nicolet 510 apparatus (Source: Globar, Detector: DTGS). This technique was employed to determine the inorganic anions and organic functional groups present in the compounds. The Nic-Plan optical microscope is coupled confocally to the spectrometer, which allows us to perform micro-FTIR on each layer of the sample. The detector is cooled by means of a liquid nitrogen trap.

A dispersive integrated Raman system, the Horiba Jobin–Yvon Labram Infinity, was employed to probe the Raman scattering. The optical microscope is coupled confocally to an 800 mm focal length spectrograph equipped with two switchable gratings. Two external visible diode lasers (solid state source) are available: one is at 514.5 nm and the other at 752.5 nm. It has a CCD detector, and the resolution is of 1800 lines/mm; the time of acquisition was 100 s in almost all the cases, and the size of the analyzed zone approximately 5 μm.

Elemental chemical analyses were obtained using a scanning electron microscope Jeol JSM5400 equipped with an X-ray dispersive energy analyzer.

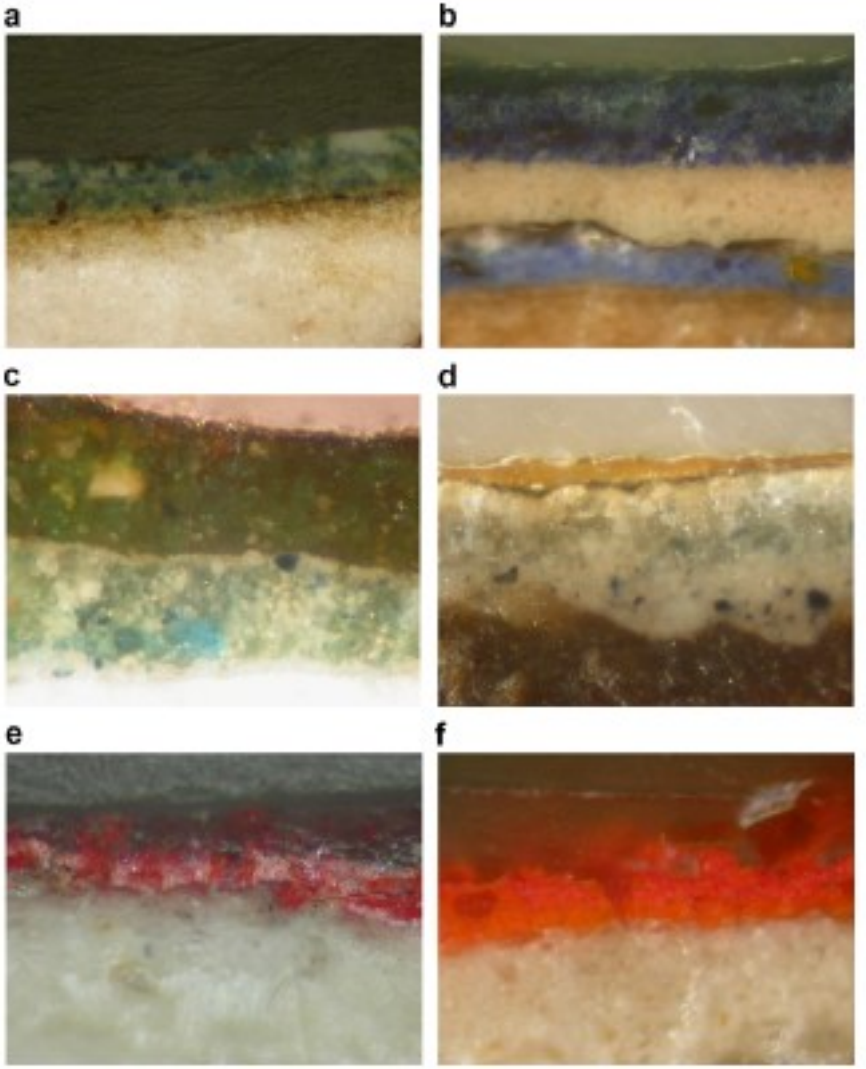

Fig. 1. Microphotographs of cross-sections corresponding to several samples studied in this work, (a) Kings' Room in Alhambra from Granada, (b) Our Lady Santa Ana, (c) El
Salvador Church, (d) Murillo's painting, (e) Kings' Room in Alhambra from Granada, and (f) Our Lady Santa Ana.

Journal of Molecular Structure 924–926 (2009) 404–412

Comparison between micro-Raman and micro-FTIR spectroscopy techniques for the characterization of pigments from Southern Spain Cultural Heritage

M.L. Franquelo [a,*], A. Duran [a,b], L.K. Herrera [a], M.C. Jimenez de Haro [a], J.L. Perez-Rodriguez [a]

In this paper, it was shown that micro-Raman, micro-FTIR and EDX are complementary techniques for the study of cross-sections of the materials constituting artworks. These techniques have permitted the characterization of blue, red, ochre, green, orange, yellow and white pigments present in polychromed sculptures, canvas, walls painting and several paintings from the Alhambra of Granada from Andalusia Cultural Heritage.

This work has proven that the study of cross-sections by micro FT-IR spectroscopy is quite a useful technique in the characterization of compounds containing inorganic polyatomic anions (most of them oxoanions), which show bands in the 'fingerprint' zone of the spectrum. On the other hand, the incorporation of micro-Raman spectroscopy into the study of the same cross-sections is very useful. We can conclude, without doubt, that this technique permits not only the characterization of the stoichiometry of the compound, but also the phase or phases in which it is present and even, in many cases, its natural occurrence or its synthetic origin. Thus, we have shown that the combined use of both micro-spectroscopies yields complementary information that is useful for the determination of pigments in works of art.

Raman spectroscopy allows the characterization of amorphous materials, and it has an advantage over powder XRD, which is only suitable for crystalline samples. Thus, it is used in the characterization of smalt, frequently used by Murillo, for instance.

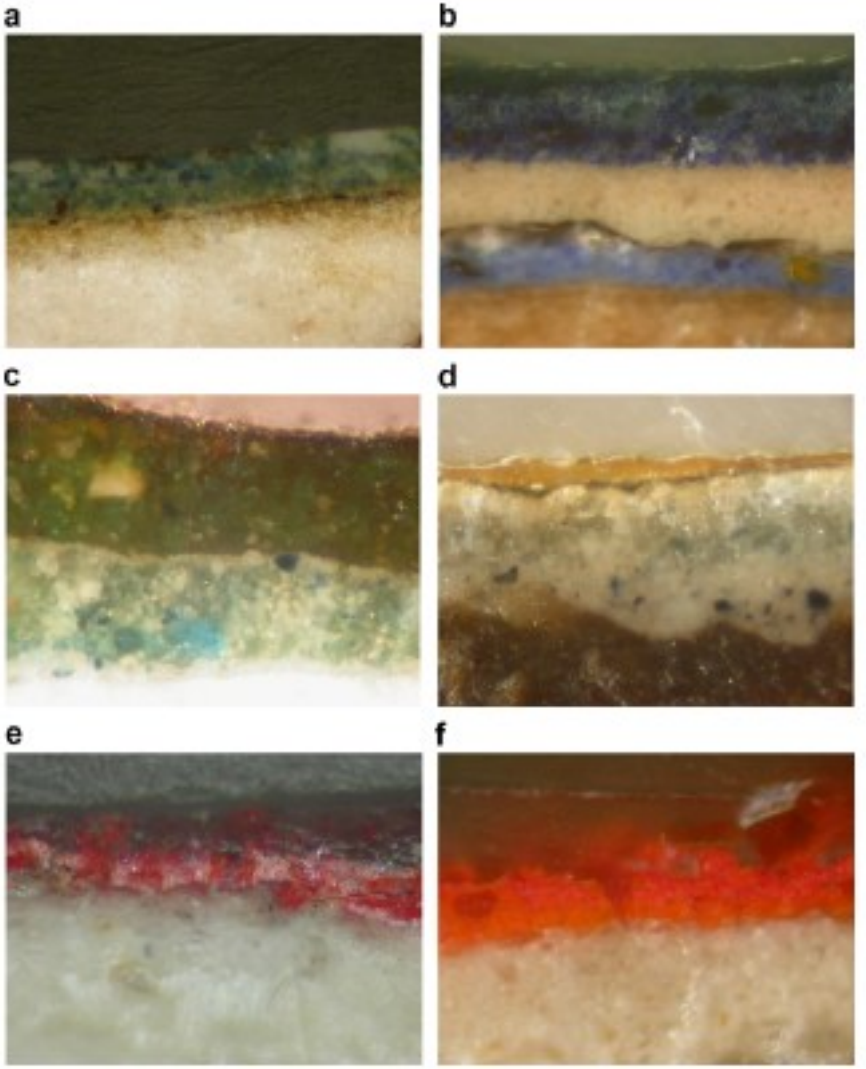

Fig. 1. Microphotographs of cross-sections corresponding to several samples studied in this work, (a) Kings' Room in Alhambra from Granada, (b) Our Lady Santa Ana, (c) El
Salvador Church, (d) Murillo's painting, (e) Kings' Room in Alhambra from Granada, and (f) Our Lady Santa Ana.

Microscopy Applications

- Small samples
- Large Samples
- Plastics
- Packaging materials
- Pharmaceuticals
- Fibers
- Trace evidence
- Contaminants
- Failure analysis
- Coatings & inks
- Electronic materials
- Migration, diffusion and aging studies
- Reverse engineering
- Art conservation
- And much more